Hydrol. Earth Syst. Sci. Discuss., 8, 9173–9227, 2011
www.hydrol-earth-syst-sci-discuss.net/8/9173/2011/
doi:10.5194/hessd-8-9173-2011

Hydrology and Earth System Sciences Discussions

Characterization of the hydrological functioning of the Niger basin using the ISBA-TRIP model

V. Pedinotti[1,2], A. Boone[1], B. Decharme[1], J. F. Crétaux[3], N. Mognard[3], G. Panthou[4], and F. Papa[3]

[1]CNRM/GAME, Météo-France, CNRS, URA1357, Toulouse, France
[2]Centre National d'études spatiales (CNES), Toulouse, France
[3]Laboratoire d'Etudes en Géophysique et Océanographie Spatiales (LEGOS), Toulouse, France
[4]Laboratoire d'étude des Transferts en Hydrologie et Environnement (LTHE), Grenoble, France

Received: 30 September 2011 – Accepted: 6 October 2011 – Published: 14 October 2011

Correspondence to: V. Pedinotti (vanessa.pedinotti@gmail.com)

Published by Copernicus Publications on behalf of the European Geosciences Union.

Abstract

During the 70s and 80s, West Africa has faced extreme climate variations with extended extreme drought conditions. Of particular importance is the Niger basin, since it traverses a large part of the Sahel and is thus a critical source of water in this semi arid region. However, the understanding of the hydrological processes over this basin is currently limited by the lack of spatially distributed surface water and discharge measurements. The purpose of this study is to use the ISBA-TRIP continental hydrologic system to explore key processes related to the hydrological cycle of the Niger Basin. The scheme accounts explicitly for the surface river routing, for the floodplains dynamic, and for the water storage using a deep aquifer reservoir. In the current study, simulations are done at a 0.5 by 0.5° spatial resolution over the 2002–2007 period using the atmospheric forcing provided by the AMMA Land surface Model Intercomparison Project (ALMIP). The model is intensively compared to in situ discharge measurements as well as satellite derived flood extent, total continental water storage changes and river height changes. The flooding scheme leads to a non-negligible increase of evaporation over large flooded areas, which decrease the Niger river flow by 15 % to 50 %, according to the observed station and the rainfall dataset used as forcing. This contributes to improve the simulation of the river discharges confirming for the need to incorporate flood representations into Land Surface Model. The model provides a good estimation of the surface water dynamics and accurately simulates the endorheic property of the Northern part of the basin. Moreover, the deep aquifer reservoir improves Niger low flows and the recession law during the dry season. This study also gives a basic estimation of aquifer recharge and of the total terrestrial water budget. The comparison with 3 satellite products from the Gravity Recovery and Climated Experiment (GRACE) is really optimistic and show a non negligible contribution of the deeper soil layers to the total storage (26 % for groundwater and aquifer). Finally, sensitivity tests have shown that a good parameterization of routing models is required to optimize simulation errors. Indeed, the modification of some key parameters has non-negligible

HESSD

8, 9173–9227, 2011

impacts on the model dynamics which gives perspectives for improving the model input parameters using future developments in remote sensing technologies such as the joint CNES-NASA satellite project SWOT (Surface Water Ocean Topography), which will provide water heights and extent at land surface with an unprecedented 50–100 m resolution and precision.

1 Introduction

Over the past 5 decades, West Africa has faced extreme climate variations with extended extreme drought conditions most recently during the 70s and 80s. In this region, precipitation is closely linked with the monsoon, and better understanding and prediction are needed for improved water resource management. With an approximate length of 4180 km (2600 miles), the Niger river is the largest river in West Africa. It starts in the Guinea Highlands in southeastern Guinea and ends in Nigeria, discharging through a massive delta into the Gulf of Guinea within the Atlantic Ocean. It is a significant source of water and food for West Africa which, as an agricultural region, is highly dependent on the water availability and management practices.

According to several studies (Coe, 1998; Andersen et al., 2005; Dadson et al., 2010), the seasonal and interannual cycle of the Niger river discharge is influenced by the hydrological processes including overland processes (precipitation, evaporation, stream flows, floods, infiltration etc.) and underground processes (groundwater and/or deep aquifer recharge). These processes are theorized to have feedbacks with the climate, rainfall variability and the carbon cycle (Houwelling et al., 1999; Matthews, 2000; Bousquet et al., 2006; Taylor, 2010b; Taylor et al., 2011). Thus, a better parameterization of hydrological processes in atmospheric general circulation models (AGCMs) is necessary to obtain a better understanding of the feedbacks with the West African monsoon. This could then potentially translate into improved water resource management and climate prediction, at least at the regional scale (Gedney et al., 2000; Douville et al., 2000a,b; Molod et al., 2004; Lawrence and Slater, 2007; Alkama et al., 2008).

HESSD
8, 9173–9227, 2011

Currently, the representation of the surface component of the hydrological cycle in AGCMs is done using continental hydrological systems (CHSs) composed of land surface models (LSMs), which provide the lower boundary conditions for heat, momentum and mass. Some AGCMs go further and include river routing models (RRMs) which are used to convert the runoff simulated by the LSMs into river discharge. RRMs transfer the continental freshwater into the oceans at specific locations (as source terms for the ocean model component). The evaluation of LSM-RRM systems is therefore a crucial task. This is generally done using offline simulations driven by atmospheric forcing which is as realistic as possible: such forcing are usually generated using a combination of atmospheric model reanalysis or short term forecasts combined with satellite-based products which are calibrated or bias corrected using gauge data (Dirmeyer et al., 2006; Sheffield et al., 2006). These simulations are then evaluated with in situ river discharge data, which does not guarantee that the spatiotemporal distribution of water storage over and under the land surface is well represented. Over West Africa especially, measurement data are difficult to access due to geographical, geopolitical and economic issues. In this context, satellite remote sensing techniques (Alsdorf and Lettenmaier, 2003; Alsdorf et al., 2007; Wigneron et al., 2003; Grippa et al., 2004) have become useful tools for hydrologic investigations. For instance, efforts have already been done to quantify the soil water content/groundwater using satellite data (Rodell et al., 2009; Grippa et al., 2011). Satellite altimetry has also been used for systematic monitoring of water levels in large rivers, lakes and floodplains and several studies have demonstrated the capability of using these sensors locally for estimating river discharge in large rivers (still limited to rivers with a width of few kilometers), including the Amazon River (Leon et al., 2006; Calmant et al., 2008; Getirana et al., 2010), the Ganges-Brahmaputra (Papa et al., 2010a) or the Lake Chad Basin (Coe and Birkett, 2004). In parallel, globally applicable remote sensing technique employing a suite of satellite observations has been developed and now provides estimates of the spatial and temporal dynamics of surface water extent at the global scale over the last 2 decades (Prigent et al., 2007; Papa et al., 2010b). In the future, the joint

HESSD
8, 9173–9227, 2011

CNES-NASA Surface Water Ocean Topography (SWOT, to be launched in 2020) mission will measure the surface water height with an unprecedented resolution of 50 m over the globe (Alsdorf et al., 2007; Rodriguez, 2009). This will enable a global scale near real time monitoring of the majority of the worlds rivers, lakes and reservoirs with spatial resolution of about one hectare (Lee et al., 2010; Biancamaria et al., 2010).

The need for a better representation of the global water budget has resulted in numerous implementations of river routing schemes into LSMs, and they vary widely in their complexity and degree of calibration. For water management applications on the watershed scale, highly parameterized, geographically specific models can be used to provide accurate estimates of streamflow and reservoir status (Zagona et al., 2001; Dai and Labadie, 2001; Habets et al., 2008). For global scale applications, however, computationally efficient, easily parameterized, comparatively simple and physically-based routing methodologies are preferable. An early influential effort at large scale routing was done by Vorosmarty et al. (1989) who prepared a river routing network for the Amazon basin at a 0.5° resolution. Runoff produced by a water balance approach was routed through the network using a linear transfer model, with flow time calculated as a function of flow length, estimated subgrid scale sinuosity, and grid scale velocities estimated on the basis of mean downstream discharge (Leopold et al., 1964). A similar linear transfer model was adopted by Miller et al. (1994) for application within the Goddard Institute for Space Studies (GISS) General Circulation Model (GCM) at the global scale. In their formulation, runoff produced by a GCM at $4^\circ \times 5^\circ$ was routed to the ocean through a $2^\circ \times 2.5^\circ$ network in which flow direction was determined by topography and velocity was a function of the slope. Because the scale of the implementation was quite coarse, slope based estimates of velocity were intentionally calculated to yield low values, providing an implicit correction for subgrid scale sinuosity and the time it would realistically take runoff to work its way through the river system. Sausen et al. (1994) implemented a linear routing scheme for the European Center Hamburg (ECHAM) GCM, with transport parameters semi-objectively calibrated to match observed flow in major gauged rivers. In a study of the Amazon River system, Costa

HESSD
8, 9173–9227, 2011

and Foley (1997) adopted the velocity estimation procedure of Miller et al. (1994). As a refinement, they estimated the sinuosity coefficient independently for each tributary within the Amazon basin, and they adjusted velocities as a function of stream order. Costa and Foley (1997) further divided runoff into surface and subsurface components and applied differential source retention times to each. Further variants on the Miller et al. (1994) approach include the global hydrological routing algorithm (HYDRA, Coe, 2000), which was implemented at a 5° resolution and included variability in surface waters, and made some adjustments to the Miller et al. (1994) method for calculating distributed velocities. Oki and Sud (1998) and Oki et al. (1999) continued this line of application through the development of the topographically corrected integrating pathways for routing models, TRIP (Total Runoff Integrating Pathways). Arora and Boer (1999) implemented a time-evolving velocity that depends on the amount of runoff generated in the GCM land grid, using Mannings equation to estimate flow velocities for a river chanel with a rectangular section. More recently, Decharme et al. (2008, 2011) used this approach to implement a flood routing scheme into the ISBA (Interaction Soil Biosphere Atmosphere)-TRIP CHS. The scheme accounts explicitly for the river routing, precipitation interception by the floodplains, the direct evaporation from the free water surface, and the possible re-infiltration into the soil in flooded areas. The regional and global evaluations of this scheme at a 1° by 1° spatial resolution emphasized the importance of floodplains in the continental part of the hydrologic cycle, through generally improved river discharges and a non-negligible increase of evapotranspiration. However, it was noticed that over some basins, including the Niger, the discharge was still overestimated (Decharme et al., 2011). A possible identified cause was that these regions might overlie large aquifers that can be relatively uncoupled to the river. The difficulty of modeling the Niger basin and the current concerns about water resource management in West Africa make the improved understanding of this basin a scientific and socio-economic challenge. The purpose of this study is to evaluate the ISBA-TRIP CHS model including a flooding scheme and a new simple aquifer reservoir, over the Niger basin using comparisons with in situ measurements as well

HESSD
8, 9173–9227, 2011

as recently available satellite derived data over the period 2002–2007, which covers the core observation period of the African Monsoon Multidisciplinary Analysis (AMMA) project (Redelsperger et al., 2006).

In this study, we first examine the routing scheme and its ability to simulate discharge simulated by LSMs from the AMMA Land surface Model Intercomparison Project (ALMIP). For this, TRIP was run in offline mode (default made with no feedbacks with LSMs) with total runoff from 11 LSMs, including ISBA, as input data in order to explore the impact of routing alone on the river discharge. Secondly, we evaluate the ISBA-TRIP CHS model, in fully coupled LSM-RRM mode and with the addition of an aquifer reservoir. The evaluation is done using a large variety of data, consisting of gauging measurements for discharge and satellite-based products such as water heights and flooded areas. The study also attempts to give quantitative estimates of the different water budget components over the basin using comparisons with the Gravity Recovery and Climate Experiments (GRACE) products. In Sect. 4, sensitivity tests were performed to determine the robustness of the model and where the greatest uncertainties exist with respect to model parameters. Finally, the ability of the model to reproduce the endorheic property of the basin is presented in Sect. 5.

2 The ISBA-TRIP model

2.1 Review of the ISBA-TRIP model

ISBA is a state-of-the-art land surface model which calculates the time evolution of the surface energy and water budgets (Noilhan and Planton, 1989). In this paper, we use the 3-layer force-restore option (Boone et al., 1999). It includes a comprehensive sub-grid hydrology to account for the heterogeneity of precipitation, topography and vegetation in each grid cell. A TOPMODEL approach (Beven and Kirkby, 1979) has been used to simulate a saturated fraction, f_{sat}, where precipitation is entirely converted into surface runoff (Decharme et al., 2006). Infiltration is computed via two sub-grid exponential distributions of rainfall intensity and soil maximum infiltration capacity (Decharme and Douville, 2006).

The TRIP RRM was developed by Oki and Sud (1998) at the University of Tokyo. It was first used at Météo-France to convert the model simulated runoff into river discharge using a global river channel network at a 1° resolution. The original TRIP model is only based on a single surface prognostic reservoir, S (kg), whose discharge is linearly related to the river mass using a uniform and constant flow velocity.

In the new ISBA-TRIP CHS, TRIP takes into account a simple groundwater reservoir, G (kg), which can be seen as a simple soil-water storage, and a variable stream flow velocity computed via the Mannings equation (Decharme et al., 2010; Appendix A). In addition, ISBA-TRIP includes a two-way flood scheme in which a flooded fraction, fflood, of the grid cell can be determinate (Decharme et al., 2008, 2011). The flood dynamics is indeed described through the daily coupling between the ISBA land surface model and the TRIP river routing model including a prognostic flood reservoir, F (kg). This reservoir fills when the river height exceeds the critical river bankfull height, h_c (m), and vice-versa (Appendix B). The flood interacts with the soil hydrology through infiltration, I_f (kg s^{-1}), and with the overlying atmosphere through precipitation interception P_f (kg s^{-1}) and free water surface evaporation E_f (kg s^{-1}). This results in a system of three prognostic equations:

$$\left|\begin{array}{l} \frac{\partial G}{\partial t} = Q_{sb} - Q_{out}^{G} \\ \frac{\partial S}{\partial t} = Q_{in}^{S} + Q_{out}^{G} + \left(Q_{out}^{F} - Q_{in}^{F}\right) - Q_{out}^{S} \\ \frac{\partial F}{\partial t} = Q_{in}^{F} + (P_f - I_f - E_f) - Q_{out}^{F} \end{array}\right. \tag{1}$$

where Q_{sb} (kg s^{-1}) is the deep drainage from ISBA, Q_{out}^{G} (kg s^{-1}) the groundwater outflow, Q_{in}^{S} (kg s^{-1}) the sum of the surface runoff from ISBA within the grid cell with the water inflow from the upstream neighboring grid cells, and Q_{out}^{S} (kg s^{-1}) is the simulated

HESSD
8, 9173–9227, 2011

Characterization of the hydrological functioning of the Niger basin

V. Pedinotti et al.

discharge, while $Q^{\mathrm{F}}_{\mathrm{in}}$ and $Q^{\mathrm{F}}_{\mathrm{out}}$ (kg s^{-1}) represent the flood inflow and outflow respectively. See Appendix A and B for more details.

The global evaluation of the ISBA-TRIP CHS model at a 1° by 1° resolution suggested that the model may not take into account some important process such as the presence of large aquifers in certain regions (Decharme et al., 2011). Also, by comparing the chemical composition of river water and groundwater, Fontes et al. (1991) demonstrated that significant aquifer recharge occurs in the Niger Inland Delta region, especially during summer flooding. For these reasons, a simple linear aquifer reservoir was added to the model. This reservoir was built on the example of the groundwater reservoir, G, but with a significantly longer time delay factor, τ_{aq} (s). This results in a new system of four prognostic equations:

$$\left|\begin{aligned} \frac{\partial G}{\partial t} &= \alpha Q_{\mathrm{sb}} - Q^{\mathrm{G}}_{\mathrm{out}} \\ \frac{\partial S}{\partial t} &= Q^{\mathrm{S}}_{\mathrm{in}} + Q^{\mathrm{G}}_{\mathrm{out}} + \left(Q^{\mathrm{F}}_{\mathrm{out}} - Q^{\mathrm{F}}_{\mathrm{in}}\right) - Q^{\mathrm{S}}_{\mathrm{out}} \\ \frac{\partial F}{\partial t} &= Q^{\mathrm{F}}_{\mathrm{in}} + (P_{\mathrm{f}} - I_{\mathrm{f}} - E_{\mathrm{f}}) - Q^{\mathrm{F}}_{\mathrm{out}} \\ \frac{\partial \mathrm{Aq}}{\partial t} &= (1-\alpha)\, Q_{\mathrm{sb}} - Q^{\mathrm{Aq}}_{\mathrm{out}} \end{aligned}\right. \tag{2}$$

where α represents the fraction of deep drainage going into the groundwater reservoir while the rest of the drainage $(1-\alpha)$ goes into the aquifer. Unlike the groundwater reservoir, we assume that the aquifer reservoir local feedbacks are negligible, but it contributes to the flow at the mouth of the river. The aquifer outflow $Q^{\mathrm{Aq}}_{\mathrm{out}}$ (kg s^{-1}) can be written as follows: $Q^{\mathrm{Aq}}_{\mathrm{out}} = \frac{\mathrm{Aq}}{\tau_{\mathrm{Aq}}}$ (3) where τ_{Aq} (s) is a constant and uniform time delay factor, which represents the time for the aquifer reservoir to drain laterally to the ocean (out of the basin). This simple approach is currently motivated mainly by the lack of data describing the water table, which would be required for a more detailed approach. Figure 1 illustrates the configuration of the ISBA-TRIP CHS model used in this study.

2.2 TRIP specific parameters

The baseline parameter values are presented in this section: the sensitivity of the model to these parameters will be investigated in a subsequent section. For the model evaluation, the time delay parameters for the groundwater and deep aquifer reservoirs are fixed to 30 days and 4 years, respectively. The aquifer parameter α is initially fixed at 3/4 (which implies that 1/4 of the drainage flows into the deep aquifer).

The river width is an important parameter because it modulates both the river flow and the floodplain dynamics. It is computed over the entire TRIP network via an empirical mathematical formulation that describes a simple geomorphologic relationship between W and the mean annual discharge at each river cross section (Knighton, 1998; Arora and Boer, 1999; Moody and Troutman, 2002; Decharme et al., 2011):

$$W = \max\left(30, \beta \times Q_{\mathrm{yr}}^{0,5}\right) \tag{3}$$

where $Q_{\mathrm{yr}}^{0,5}$ ($\mathrm{m}^3\,\mathrm{s}^{-1}$) is the annual mean discharge in each grid cell estimated using the global runoff database from Cogley (1998). As discussed in Decharme et al. (2011), the β coefficient can vary drastically from one basin to another (Knighton, 1998; Arora and Boer, 1999; Moody and Troutman, 2002). Decharme et al. (2011) proposed that β varies according to climatic zone and fixed β to 20 for monsoon basins and to 13 for semi-arid and arid basins. As the Niger river flows through both such climate zones, two different values are used within the Niger basin: β is 20 for the branch of the river going from the river mouth (5° N) to 12° N and β is fixed to 10 for the remaining branch of the river. The spatial distribution of the river width is shown in Fig. 3a.

The key parameter for the floodplain parameterization is h_c, the critical river bankfull height (Decharme et al., 2008, 2011). In this study, as proposed by Decharme et al. (2011), it is computed according to the river width via a simple power function: $h_c = W^{1/3}$ (5) The spatial distribution of h_c is shown in Fig. 3b. However, owing to both the uncertaintities in this parameter and its impact on model results, sensitivity

HESSD
8, 9173–9227, 2011

tests will be carried out using arbitrary $h_c \pm 20\,\%$ (Decharme et al., 2008) leading to an increase or decrease in bankfull height up to 2m.

Finally, as discussed and proposed by Decharme et al. (2010), the Manning friction factor n_{riv} varied linearly and proportionally to W from 0.04 near the river mouth to 0.1 in the upstream grid cells (Fig. 3c): $n_{riv} = n_{min} + (n_{max} - n_{min}) \left(\frac{W_{mouth} - W}{W_{mouth} - W_{min}} \right)$ (6) where n_{riv} represents the Manning n factor of the grid cell, n_{max} and n_{min} the maximum and the minimum values of the Manning friction factor (respectively equal to 0.1 and 0.04), W_{min} (m) the minimum river width value and W_{mouth} (m) the width of the mouth in each basin of the TRIP network.

3 Model setup and experimental design

3.1 Methodology

In order to determine the impact of the flooding scheme on simulated discharges, the TRIP routing model is used in offline mode, uncoupled from a LSM and without floodplains. ALMIP I, which is a part of the AMMA project, was motivated by an interest in fundamental scientific issues and by the societal need for improved prediction of the West African Monsoon (WAM) and its impacts on West African nations (Redelsperger et al., 2006). As part of this project, ALMIP I focused at better understanding land-atmosphere and hydrological processes over western Africa (Boone et al., 2009). LSMs were run offline with prescribed atmospheric forcing consisting in a combination of observations, satellite products and atmospheric model output data. All of the LSMs used the same computational grid at a 0.50° spatial resolution (see the domain on Fig. 2). The advantage of using ALMIP data is that each LSM can simulate a different runoff response, therefore we use an ensemble of inputs. In the current study, 11 simulations are used over the 2002–2006 period. TRIP is used to compute daily outputs of discharges along the river and water mass storage for each activated reservoir.

HESSD
8, 9173–9227, 2011

In addition, the ISBA-TRIP CHS coupled model is used with and without the flooding scheme to quantify the impact of the scheme on the discharge and the surface energy budget. In the second part of this study, the deep aquifer reservoir is implemented into the ISBA-TRIP CHS model and deep drainage water is then distributed between deep soil layers and this aquifer reservoir (see details in Sect. 2). Comparison with both in-situ and remote sensing data will allow us to evaluate the simulated surface processes and the impact of the inclusion of floodplains, and to obtain an estimate of the aquifer annual recharge and river discharge.

3.2 Atmospheric forcing dataset to run ISBA-TRIP

The atmospheric state variables are based on the European Centre for Medium Range Forecasts (ECMWF) ECMWF numerical weather prediction (NWP) model forecasts for the years 2002–2007. The forcing variables consist in the air temperature, specific humidity, wind components at 10 m, and the surface pressure, all at a 3 h time step. Because of the importance of having accurate incoming radiation fluxes and precipitation, and because of the potentially significant errors in these variables derived from NWP models over this region (e.g. see Boone et al., 2009), merged satellite products are used. The downwelling longwave and shortwave radiative fluxes are provided by the LAND-SAF project (Geiger et al., 2008). Two products are used for rainfall forcing. The TRMM 3B42 product (Huffman et al., 2007) is used by default.

However, several studies have shown that RFE2 produces rainfall over the Sahel agrees better with observed values than the other available rainfall products (Pierre et al., 2011), but it is at a time step which is not well adapted to land surface modeling (daily time step). Therefore, a second set of rainfall forcing data was created using the RFE2 (Laws et al., 2004) daily rainfall product: the original rainfall is renormalized such that it produces nearly the same monthly averages as RFE2, but the temporal disaggregation to 3 h time steps is done using the aforementioned TRMM product. This re-normalized rain forcing is referred to as RFE-Hybrid (RFEH) herein. Because the simulations with TRMM-3B42 forcing were generally not as good as those using the

RFEH rainfall, the TRMM dataset will be used to run ISBA-TRIP, only for the comparison with ALMIP models discharge (to be coherent with the ALMIP project methodology). However, all the following studies and evaluations will be done using the RFEH dataset as rainfall forcing.

3.3 Evaluation datasets

Over the evaluation period (2002–2006), the simulated discharges are compared with daily gauge measurements along the Niger river from the Niger Basin Authority (ABN) as part of their Niger-HYCOS Project. These data are available in Kandadji, Ansongo and Niamey. Monthly discharge data from the Global Runoff Data Center (GRDC; http://www.grdc.sr.unh.edu/index.html) are also available in Lokoja and Malanville (see Fig. 2).

Satellite-derived inundation estimates are used to evaluate the spatial distribution and the time evolution of the flooded areas. Two different products are used. The first product is based on data from the MODIS multispectral imaging system installed onboard the Terra and Aqua satellites. In this study, the surface reflectance product (MOD09GHK) is used which is defined as the reflectance that would be measured at the land surface if there were no atmosphere. The spatial resolution is 500 m for the corresponding MODIS images. In order to detect open water and aquatic vegetation in arid and semi arid regions, a classification is performed using the fact that water surfaces do not reflect in the visible and near infra-red part of the spectrum. A threshold value has been estimated for reflectance in the MODIS frequency band-5 1230–1250 nm and for the NDVI index (Table 1) in order to delineate the shallow, sediment laden, and open water over the Inner Niger Delta, and also in order to distinguish between aquatic vegetation and that on dry land. It has been assumed that small values of surface reflectance in band-5 characterize open water, independent of the NDVI index. When the surface reflectance in band-5 increases to the median value, depending on the NDVI index, it is assumed that there is a partial coverage of dry land by water, aquatic vegetation or vegetation on dry land. Finally, dry land is assumed when

HESSD
8, 9173–9227, 2011

the NDVI is small and surface reflectance in band-5 is large. NDVI has been shown to be a robust index for monitoring temporal changes of the vegetation photosynthetic activity (Lyon et al., 1998; Lunetta et al., 2006). In the arid environment, a high level of vegetation photosynthetic activity can only be sustained by the presence of surface water or groundwater discharge. If dense enough, the aquatic vegetation and hydrophilic plants can mask underlying water and should be included in the estimate of the total area of the floodwaters. The NDVI ranges from negative values (open water) to >0.5 for dense vegetation.

The second product consists in global estimates of the monthly distribution of surface water extent at about 25 km sampling intervals. These data were generated from complementary multiple satellite observations, including passive (Special Sensor Microwave Imager) and active (ERS scatterometer) microwaves along with visible and near infrared imagery (advanced very high resolution radiometer; AVHRR). These estimates were first developed over 1993–2000 (Prigent et al., 2007), adjusted and extended over 1993–2004 (Papa et al., 2010b) and recently recomputed for the entire period 1993–2007. This dataset has been extensively evaluated at the global scale (Papa et al., 2010) and at river basin scale, including the Niger River (Papa et al., 2008). In the present study, this dataset is aggregated to a 0.5° resolution and referred to as PP. Because PP does not make distinction between the diverse anthropogenic and/or natural water bodies while the ISBA-TRIP output must be compared only with flooded areas, two additional datasets are used to hybridize PP in order to conserve information on flood inter-annual variability only: the Global Lakes and Wetland Database (GLWD; Lehner and Döll, 2004) and the Monthly Irrigated and Rainfed Crop Areas (MIRCA2000; Portmann et al., 2010) database. The corresponding final product is named CPP in this study. The methodology is described in detail by Decharme et al. (2011), and so it is not detailed here.

Water height changes over the basin are evaluated using the HYDROWEB hydrological database (http://www.legos.obs-mip.fr/en/equipes/gohs/resultats/i_hydroweb). The water level time series are based on altimetry measurements from ENVISAT satellite.

Seven sites were chosen for the evaluation, one upstream of the Niger inner delta, four downstream of the delta and two in the delta. The data are available at a regular 35 days time step (with occasional missing data) from November 2002 to the end of 2006 (Calmant et al., 2008).

Total Water Storage (TWS) variations over the entire basin are evaluated using data from the Gravity Recovery and Climate Experiment (GRACE; Tapley et al., 2004). GRACE provides monthly TWS variation estimates based on highly accurate maps of the earth's gravity field at monthly intervals at a resolution of approximately 300–400-km (Wahr et al., 2004; Swenson et al., 2003). The instrumentation and onboard instrument processing units are described in detail in Haines et al. (2003). Here, we used 48 months (from January 2003 to December 2006, excluding June 2003 and January 2004 because products are not available) of the Release 04 data produced by the Center for Space Research (CSR at The University of Texas at Austin), the Release 4.1 data produced by the Jet Propulsion Laboratory (JPL), and the GeoForschungsZentrum (GFZ) Release 04 (more details concerning GRACE data are available online at http://grace.jpl.nasa.gov/data/). The combination of these data with those datasets described in the previous paragraphs above will allow us to evaluate the distribution of water in the different TRIP reservoirs and to have a first estimation/validation of the aquifer water storage variations.

4 Results

4.1 Improvement of simulated discharges due to river flood

The evaluation of the simulated river discharge is important for hydrological applications as well as for climate studies. Previous studies (Coe et al., 2008; Decharme et al., 2008, 2011; Dadson et al., 2010) have shown that the inclusion of a flooding scheme can impact the hydrological cycle by increasing the average evaporation and reducing the simulated discharge, which leads to a better estimation of the latter. Indeed, while

HESSD
8, 9173–9227, 2011

an increasing number of LSMs used for large scale hydrological or GCM applications use river routing, most of these models do not represent floodplains. Flooded zones can be significant sources of evaporation and have a role of surface water keepers, and their exclusion can result in an overestimation of the discharge for basins with significant annual flooding. To generalize this result, the TRIP RRM model was used in offline mode and without the flooding scheme (or aquifers), to convert simulated runoff and drainage from 11 LSMs into discharge. The LSMs considered for this study were part of the ALMIP I project (Boone et al., 2009). The Fig. 4 shows the mean monthly discharges simulated by the ALMIP models (black line) for several locations along the river. The blue range is the difference between the minimum and the maximum value of discharges simulated by the models and the red line is the observed discharge. All of the ALMIP land surface models clearly overestimate the discharge. In Malanville, the mean simulated discharge is around 5 times higher than that observed over this period. At the other sites (Niamey, Kandadji, Ansongo, and Lokoja), the mean simulated discharge is 2 to 2.8 times higher than observed. However, the variability of the discharge is well captured by the models with a correlation going from 0.59 (Kandadji) to 0.85 (Lokoja) over the period. The green line represents the discharge simulated by the ISBA-TRIP CHS model with the flooding scheme activated. The discharge decreases considerably with a reduction of 50 % in Niamey, Kandadji, Ansongo and Malanville and 26 % in Lokoja. Indeed, part of the water in the floodplains evaporates, while part infiltrates into the flooded soil thereby reducing the stream reservoir water storage and discharge. The Nash-Sutcliffe coefficient or efficiency (eff) is also improved.

Figure 5 shows the monthly discharge simulated by ISBA-TRIP when forced by the RFEH rainfall dataset with and without using the flooding scheme. Indeed, as said in the methodology section, the RFEH rainfall dataset generally giving better simulated discharges, it was used for the upcoming evaluations. Here again, the activation of the flooding scheme reduces the discharge by 15 % (Lokoja) to 45 % (Ansongo). The efficiency is further improved by the flooding scheme compared to the previous simulation forced with the TRMM rain product. In fact, the dry season is better simulated

HESSD
8, 9173–9227, 2011

using this forcing dataset. However, the model still has a difficulty simulating the discharge behavior during the low flow season. In fact, the discharge remains relatively high during the dry season compared to the observations which implies that there is too much water in the river. Several reasons for this can be identified, such as underestimated evaporation, an underestimation of the water in flooded areas or the neglect of aquifers. Anthropologic activities (dams, agriculture and water use for domestic consumption) are not precisely quantified and can also explain the bias between observed and simulated discharge especially during the dry season when the population might need to extract more water from the river due to the lack of rain. The next section will show the improvement of the low flow season modeling owing to the consideration of deep aquifer storage. The impact of the flooding scheme on the surface energy budget was also investigated where the total evaporation includes evaporation from the soil and flooded areas and transpiration. The flooding scheme contributes to an increase in the evaporation mainly over the inland delta and in the southern part of the basin (+280 % with TRMM rainfall and +200 % with RFEH) which are areas which generally experience significant floods (see Sect. 5.2.b). These results emphasize the importance of modeling flood-feedbacks over regions with seasonal flooding such as the Niger delta region.

4.2 Impact of a deep aquifer reservoir and estimate of aquifer recharge

As already said, a fourth reservoir was added to the ISBA-TRIP model to represent deep aquifer processes (Sect. 2). Indeed, the model simulates too much water in the river that could be due to the presence of large aquifers (Fontes et al., 1991; Decharme et al., 2011). Different values of the aquifer recharge factor (1-α) were tested and only the most relevant result is kept for the evaluation (see sensitivity tests in Sect. 6 for further details).

The introduction of an aquifer impacts the discharge mostly on its descending phase by reducing the low flow but deteriorating the period except in Lokoja where the period and the recession law are improved (Fig. 6). The reduction of low flows is explained

HESSD

8, 9173–9227, 2011

by the fact that the river empties faster after the rainy season which results to a more realistic discharge during the dry season. In terms of statistics, the scores (ratio, rmse, eff) are similar or slightly deteriorated except in Malanville and Lokoja where they are improved (relative bias is 0.31 without aquifers and reduced to 0.04 with aquifers). The correlation score, however, is improved at all of the sites. In addition to improving the recession law, the aquifer contributes to a decrease in surface evaporation by 6 to 16 % for the main flooded regions (Fig. 7) since there is less water at the surface available for evaporation. The sensitivity of the model to the choice of the time delay factor τ_{Aq} and the fraction α will be presented in Sect. 5.

Vouillamoz et al. (2007) used magnetic resonance sounding to give recharge estimate in semiarid Niger in order to better constraint hydrogeological models. If this method presents some uncertainties, they showed that it remains useful for characterizing the unconfined aquifer of south-western Niger. In this study, the aquifer recharge rate (recent rate due to vegetation clearance) is estimated to be 23 mm 5 mm per year. The ISBA-TRIP CHS gives a mean aquifer recharge rate of 26 mm per year over the period of simulation 2002–2006 which is coherent with the study of Vouillamoz et al. (2007). Even if the estimate from Vouillamoz et al. (2007) was done over a much smaller area than in this study, this result emphasizes the ability of the model to distribute the water between the different hydrological components. This result shows the need for representing aquifer processes in the model to get a more realistic water distribution in the basin.

4.3 Flooded areas

The quantification of wetland extent is an important step towards a better representation of surface water dynamics. In this study, the time and spatial distribution of wetlands were evaluated over the inner delta region, which is a large inundated area, and over the whole basin. Figure 8a and b show the time evolution of the mean monthly flooded fraction (in %) averaged over the inner delta region and over the Niger basin, respectively. The blue range on the Fig. 8a represents the interval between the minimum

HESSD
8, 9173–9227, 2011

and the maximum Modis derived (JFC) flooded fraction. The simulated flooded fraction is generally included in this range although it tends to be on the low end. This is reasonable since the Modis classification (JFC) fraction includes wetted vegetation an near-surface saturated soils. However, as shown in the figures, the CPP product is around 3 times higher than the modeled values over the basin and 10 times higher over the delta. This can be explained by the fact that the multi-satellite method can encounter some difficulties in accurately discriminating between very moist soils and standing open water and likely overestimates the actual fraction of inundations (Papa et al., 2010a,b).

Figure 8c and 8d show the time series of de-seasonalized anomalies (obtained by subtracting the 12-year mean monthly value from individual months and then divided by the standard deviation) over the delta and over the basin. Over the delta, the Fig. 8c suggests that the model and the data are in good agreement in their time variations, with a better phasing between CPP and ISBA/TRIP. Over the basin, the CPP and model anomalies globally corroborate in phase and amplitude.

The spatial distribution of the inundated areas, as well as their seasonal variability, are well represented by the model. Indeed, for both of the CPP products and the simulation, the most important inundations occur between August and October and over two main regions, i.e. the inner delta in Mali and in the eastern part of the basin at the border between Niger and Nigeria.

4.4 River height change

To complete the evaluation of surface water dynamics, the river height time changes are compared to estimates from the HYDROWEB hydrological database developed by the LEGOS/GOHS (Calmant et al., 2008) which gives estimations of height changes at several points along the Niger river (Fig. 9). The seven locations used for comparison are noted in purple in Fig. 2. The bias error on the HYDROWEB water levels measures is estimated to be around 20 cm and the peaks of water height changes are within a range between 2 and 4 m. Since our interest is to be able to reproduce extreme events, this error is considered as reasonable for evaluating water height changes. Globally, the water height changes are well represented by the model, with a slight phase delay for location 2. The model also overestimates the peaks of positive height changes which might be due to forcing anomalies (rain) or to model deficiencies. Indeed, the surface runoff stream function might be false in some areas and, if overestimated, results in an overestimation of water height variation during rain events. Also, uncertainties in the river bed slope can also result in an overestimation of the water height changes in the valleys. However, no attempt is made to calibrate these parameters here, which would be a long and difficult process and which is not necessary for use in a GCM.

4.5 Total terrestrial water storage

Figure 10 shows the comparison between 3 GRACE satellite products that estimate the total water storage (TWS) change globally at 1° resolution (the blue range in the lower panels represents the difference between the maximum and minimum monthly observation values) and the water storage change in all of the reservoirs of the ISBA-TRIP model, averaged over the basin. The left panels represent the inter-annual variations (monthly means) and the right panels are the intra-annual variations (2003–2006 average for each month). The blue curve on the lower panels represents the mean water storage change of the Niger basin in all of the ISBA-TRIP reservoirs. The upper panels contain the water storage change in each reservoir (averaged over the basin) and the middle panels present the time evolution of the rain, drainage, runoff and evaporation over the basin. The comparison of ISBA-TRIP water storage change with the GRACE products over the Niger basin shows a good correlation between the simulation and observations. The contributions of each reservoir to the total water storage change appear in the legend. Although the uppermost soil layers (approximately 1 to a few meters) comprise most of the total water storage change over the basin (56 %), the contribution of the other reservoirs, such as the groundwater and the aquifer, are not negligible (12 % and 14 %). The contribution of flooded zones is less (3 %), but since their impact on evaporation is not negligible they must be considered also. These

HESSD
8, 9173–9227, 2011

results emphasize the need for considering all such reservoirs in LSMs in order to close the water budget. Generally, studies compare the GRACE water storage change to the water storage change in the hydrologic soil layers only i.e. the first soil meters (green curve in the last panel). However, this approximation is likely less valid for regions with significant storage in flooded zones and deeper soil layers since the contribution of these two reservoirs to the total water storage is no more negligible.

4.6 Sensitivity tests

Sensitivity tests were performed to determine the input parameters which have the most significant impact on the simulations. For global simulations, it is preferable that the model is not sensitive to too many parameters since tuning is a long and fastidious process at the global scale and spatially distributed global scale observational data is currently rather limited. Generally, physiographic relationships or the derivation of secondary parameters are preferred. The sensitivity of the ISBA-TRIP model to several key input parameters was investigated in this study. The Table 1 presents the key input parameters and the variations applied.

We first investigate the impact of the river critical height, hc, on the simulated discharge. The river width W is kept the same as in previous simulations. Increasing the critical height by 20 % leads to 5 % less flooded fraction over the inner delta and in the south of the basin. The evaporation also decreases over the flooded zones by 4 to 12 % (relative bias). Conversely, when decreasing the river height by 20 %, the flooded fraction is 5 % more over the same areas and the evaporation is increased by 14 to 24 %.The water height changes are also influenced by the critical height modification. Over the 7 virtual sites, an increase of h_c globally increases the water height changes (+30 %), while a decrease of h_c decreases the water height changes (−16 %). This can be explained by the fact that a river with a small h_c will be flooded earlier and the water will spread more rapidly over the surrounding area, making the river water level less sensitive to rain events. In terms of inter-annual discharge, increasing or decreasing h_c, respectively, increases or decreases the amplitude of the discharge by 5 to 15 %

(Fig. 11a and b). However, the annual variability of the discharge is not changed by a modification of the critical height. In Niamey, Ansongo and Kandadji, the increase of h_c leads to better statistical scores which might suggest that the model overestimates the inundations in these areas. In contrast, in Malanville, the scores are better when reducing the critical height which suggests an underestimation of flooding at this site. In Lokoja however, the scores are better for the standard simulation. The impact of the river width, W, was also investigated. The critical height is not changed. Increasing W increases the amplitude of the discharge by around 6 % while decreasing arbitrary W by 20 % decreases the discharge by 9 % (Fig. 11c and d). The water height changes vary differently according to the site. For example, for location 1 (see Fig. 2 for locations) a 20 % reduction of the river width reduces the mean water height changes by 35 % over the studied period. However, for locations 2, 4, 5, 6 and 7 the mean water height changes increase by 15 % to 28 % and there is no change for location 3. Indeed, water height changes depend on the topography which is modified with river width variations. Evaporation over the flooded areas is reduced by 3 to 9 % when W increases and increased by 4 to 16,% when W decreases. There are no significant impacts of W and h_c on the total water storage change. Indeed, the storage of the different reservoirs and the amount of drainage are only slightly changed by the modification of these parameters.

The mean value of the Manning coefficient is around 0.075 and the frequency distribution of the Manning coefficient shows that most of the pixels have values above 0.06 (91 out of 110). As the Niger basin covers a large area, the soil properties are very heterogeneous all over the basin, making it necessary to use spatial distributions of soil parameters. Two new distributions of n_{riv} were created and used to run the model: one distribution in which n_{riv} coefficient is arbitrary reduced by 40 % and the other one in which it is increased by 20 %. In order to keep a value included in a reasonable range (between 0.03 and 0.1) all the values out of this range after modification are set equal to the closest value in this range. Figure 12a shows the behavior of the discharge for each distribution of n_{riv}. Increasing the Manning coefficient delays the response of

HESSD
8, 9173–9227, 2011

Characterization of the hydrological functioning of the Niger basin

V. Pedinotti et al.

the river to rain events. Indeed, small values of the coefficient speed the rise in water level and increase discharge amplitude. Also, the decrease of the discharge after the rainy season is faster when n_{riv} is smaller. We can also notice that when n_{riv} is bigger, the model is better able to dissociate the different rain events and two peaks of discharge appear. Flooded areas and evaporation are higher for large values of n_{riv} as the water flows more slowly in the river bed, generating smaller river height changes, and flooded areas empty to the river more slowly. The evaporation increases by 14 % over main evaporation areas when n_{riv} is 20 % higher and decreases by 18 % when it is 40 % smaller. Flooded areas are 15 % higher over the inner delta area when the Manning coefficient increases and 30 % smaller when it decreases. The increase of n_{riv} also delays the water height changes while small values of n_{riv} decrease the peaks of river height changes. However, the impact of this coefficient on the water height change is more or less significant according to the observation sites and for most of them this impact is not obvious. Finally, these modifications of n_{riv} have no significant impact on the total water storage change. Thus, the current distribution used in the model is the most reasonable according to the scores.

5 Endorheism of the northern Niger basin

The monitoring of the Niger basin started in 1907 when two observation stations were built in Koulikoro, Mali and in Jebba, Nigeria. The current observation network contains about 200 stations and has improved the general knowledge of the hydrological functioning of the basin. The 2005 annual report of the World Bank Group underscored the endorheic property of the northern part of the Niger basin, where surface runoff and stream flow do not reach the river (Andersen et al., 2005). This endorheic area covers almost half of the area of the Niger basin (Fig. 13a, from Descroix et al., 2009). Figure 13b represents the ratio of the sum of the runoff and drainage calculated by ISBA, over the precipitation. This ratio is averaged over the period 2002–2007 for each pixel of the basin. The ratio is nearly zero in the northern part of the basin which means that there is almost no runoff or drainage in this area and thus no water flowing to the river simulated by the model. Moreover, the dark blue pattern on Fig. 13b (corresponding to a ratio inferior to 0.1) is close to the pattern of the endorheic region from Descroix et al. The ratio of evaporation over precipitation is superior to 0.9 (Fig. 13c) in this region which means that most of the water from precipitation evaporates. The land surface model is then able to qualitatively reproduce the endorheic behaviour of the northern Niger basin without modification of the scheme or the input parameters.

6 Discussion

The results suggest that the coupled land surface and river routing model provides a reasonable estimation of inland hydrological processes of the Niger basin when the flood scheme is activated and a deep aquifer is considered. The flooding scheme contributes to decrease streamflow and increase evaporation over flooded areas. The impacts of floods on the water fluxes and storage terms are found to be coherent with other studies (Coe et al., 2008; Decharme et al., 2008, 2011; Dadson et al., 2010) and emphasize the need for representing these processes in GCMs.

Several diverse datasets have been used for model evaluation such as river discharge, spatial and temporal evolution of flooded areas and water height changes measured by satellite (see Sect. 5). These data provide constraints for estimating the sub-surface water storage and dynamics, but also the shallow soil water content and the groundwater storage which are linearly related to the surface water. With three reservoirs out of four being constrained by measurement data, the GRACE total water storage dataset permits a preliminary estimation of the water storage change in the aquifer reservoir. Moreover, the aquifer reservoir recharge rate has been later found to be coherent with the estimate from Vouillamoz et al. (2007) which is a valuable result for the validation of the water cycle simulation. This is of interest since there are hardly any global measurements of aquifer recharge and/or discharge. If the aquifer reservoir is not found to be significantly impacting the discharge (though reducing low flows), its contribution to the total water budget is not negligible and thus, the consideration of aquifer processes is necessary to better distribute water between the water cycle components.

Evapotranspiration is the remaining water budget component, but large scale observations are not available. The evaluation of this variable has been done within the context of several other studies. The ISBA surface temperature was evaluated using brightness temperatures from AMSR (deRosnay et al., 2009) which is related to the surface energy budget and near surface soil moisture, and the monthly sensible heat fluxes aggregated from local scale observations to the ALMIP grid square were evaluated for a semi-arid region within the Niger basin (net radiation was imposed, thus monthly Bowen ratios can be estimated; Boone et al., 2009). Finally, regional scale water budget studies were performed over West Africa using ISBA evaporation estimates (Meynadier et al., 2010): all of the aforementioned studies imply that monthly scale evaporation estimates are reasonable.

Moreover, Mahe et al. (2009), estimated the water losses of the inner delta of the Niger river and their evolution from 1924 to 1996. They estimated the total evapotranspiration from the delta to be about 800 mm yr^{-1} over the period 1924–1996, varying between 400 mm yr^{-1} (1984) and 1300 mm yr^{-1} (1924). The total evapotranspiration calculated by ISBA over the period 2002–2006 is 662 mm yr^{-1} which is contained in the range estimated by the previous study. They also related the water losses in the delta to the expansion of the floodplains, highlighting the importance of considering floods in a LSM.

Sensitivity tests have shown that a good routing model is required to optimize the simulation errors. For example, Fig. 11 shows that while increasing h_c in the delta region (Niamey, Kandadji, Ansongo) would improve the simulation score, it would have the opposite effect in Malanville. Thus, improvements in remote sensing technologies should help to get maps of spatial and temporal evolution of inland waters (river width, flooded areas expansion, river height) and thus compensate the lack of in situ measurements. These data will then either be used as input data and replace geomorphologic relations used currently to describe these parameters, or they will either be assimilated into the model to correct simulation errors.

In GCMs, the input parameters, such as the Manning coefficient, critical height, river width and depth are defined by empirical relationships which might not give the best results for all modeled basins, however the objective is to give the best overall global results. However, for regional or basin scale studies, these relationships lead to non-negligible known errors which could be reduced using satellite data. Indeed, satellite data could be used to spatially distribute parameters by basin and then could contribute to the development of a global database describing the major river characteristics, at least as the stream width and the river bankfull height. This is an important step if GCM climate scenario output is to be used for water resource management at the regional scale.

We also investigated the impact of increasing the groundwater reservoir's time delay factor on discharge, which extends the time of exchange between the groundwater reservoir and the river. Decharme et al. (2010) estimated that a time delay factor of the order of 30–60 days is generally suitable for global simulations. The increase of τ impacts the discharge on the descending phase by deteriorating the recession law. The scores are not significantly changed by the increase of τ. The total water storage is not highly dependant on τ either (the mean variation represents about 5 % of the mean water storage change). However, previous results emphasized that this parameter is important since it increases the residence time of water storage in the basin and allows a more realistic simulation of the discharge.

The aquifer reservoir time delay factor has also no impact on the discharge as aquifers are assumed to be too deep and too slow to impact directly the river discharge. Modifications of τ_{Aq} have a negligible impact on the total water storage of the basin (the mean variation represents less than 10 % of the mean water storage change). However, the simulation is done over a relatively short period (5 years) over which the aquifer time delay factor might be less significant. Over longer periods of time, as for example for climatic studies, it is possible that the discharge of aquifers into

HESSD
8, 9173–9227, 2011

the ocean has a significant impact on the water budget, and thus τ_{Aq} could be one key parameter contributing to the water balance.

Input rainfall uncertainties can also be the cause of biases in the simulations as shown in Sect. 4.1 where the model, forced by two different rain datasets gives significantly different results. In this paper, only the TRMM-RFE2-hybrid rain dataset, RFEH, resulting in better simulation results was used for the bulk of the validation. However, other rain datasets were used as input rainfall to run the ISBA-TRIP model, such as PERSIANN (Precipitation Estimation from Remotely Sensed Information using Artificial Neural Networks, http://chrs.web.uci.edu/persiann/) from the Center for hydrometeorology and remote sensing (CHRS) and CMORPH (CPC MORPHing technique, http://www.cpc.ncep.noaa.gov/products/janowiak/cmorph.shtml) from the United States National Oceanic and Atmospheric Administration (NOAA). The results of the simulations using both of these rainfall datasets showed a significant overestimation of the discharge (about 5 times higher than with the RFEH forcing for both CMORPH and PERSIANN forcing and twice higher for the TRMM forcing) at all discharge observation sites even with the representation of floods and aquifers. This is consistent with the work of Pierre et al. (2011) who showed that CMORPH dataset clearly overestimates precipitations over the Sahel.

7 Conclusions and perspectives

This study describes the evaluation of the ISBA-TRIP Continental Hydrologic System (CHS) over the Niger river basin, using a prognostic flooding scheme and a linear deep aquifer reservoir. The simulations are done at a 0.5° by 0.5° resolution over the 2002–2006 period. The flood scheme accounts explicitly for the precipitation interception by the floodplains, the direct evaporation from the free water surface and the possible re-infiltration into the soil. The deep aquifer reservoir has no feedback with the river locally and drains water to the river mouth over a comparatively long timescale. The model has been developed for use in climate model applications (coupled to the

ARPEGE RCM and GCM at Meteo France) where the representation of processes such as evaporation from the continental surface and freshwater fluxes to the ocean are crucial. The evaluation is done using a large variety of data, consisting of gauging measurements and satellite-derived products. This allows the spatially distributed evaluation of the separation of the water storage into its different components and it gives a first estimate of aquifer dynamics over the basin.

Considering the relative simplicity of the routing channel, the model provides a good estimation of the surface water dynamics: the spatio-temporal variability of the flooded areas, the river discharge and the river water height changes. The flooding scheme leads to an increase of evaporation and reduction of discharge testifying for the need to incorporate flood representations into Land Surface Models (LSMs). The aquifer reservoir impacts the representation of both low flows and the recession law during the dry season. The comparisons with GRACE total water storage change (GFZ, CSR and JPL) were used to evaluate the distribution of water between the different reservoirs of the system (river, floodplains, shallow soil layers, groundwater and aquifers), and good overall agreement of total water stored with GRACE was found. It is also shown that model results compare best with GRACE when storage estimates from aquifers, rivers and flooded zones are included along with soil moisture.

Despite the fact that the main features of the river dynamics and water budget terms are represented reasonably well by this relatively simple system, some simulation deficiencies remain. For example, the model has a difficulty in terms of reproducing the discharge during the low flow period or the second annual peak of discharge. These deficiencies might be due to precipitation uncertainties or LSM errors (in terms of subgrid runoff, evaporation and soil water transfer physics, input LSM physiographic parameters such as vegetation indicies, soil texture and depth, ...): but the focus in this study is mainly on river, floodplain and aquifer dynamics. Precipitation uncertainties were briefly touched upon by using different input forcings, but few currently available rainfall products are good enough to be useful for hydrological modeling studies over this region (notably owing to large biases). Regarding the RRM errors, Decharme et al. (2011) have discussed the questionable aspects of the flooding scheme such as the empirical computation of the river width, the choice of the river bankfull height, the simplified geometry of river stream and flood reservoirs, or the use of the Manning's formula for computing the mass transfer between them. Moreover, sensitivity tests have shown the non-negligible impact of some of the parameter values on simulations. However, the model has been developed for global climate applications at low resolutions and must be as robust as possible to be applicable at global scale, and therefore has a limited number of tunable parameters. However, upcoming advances in remote sensing technologies should permit an optimization of the spatially distributed parameters of the model. In fact, forcing uncertainties, especially rain uncertainties, represent a limitation for model tuning at this scale. Moreover, they can compensate the non-representation of lakes and large ponds.

A global database describing the basin characteristics such as the river width and the bankfull height would be of great interest for improving the model simulations. This likely depends heavily on advances in remote sensing technologies, which should help to get maps of spatial and temporal evolution of inland waters (river width, flooded areas expansion, river height ...) and thus compensate for the lack of in situ measurements at the global scale. The joint CNES-NASA satellite project SWOT will provide water heights and extent at land surface with an unprecedented 50–100 m resolution and precision (centimetric accuracy when averaged over areas of 1 km; Durand et al., 2010). These data will then either be used as input data and replace geomorphologic relations used currently to describe surface parameters, or they will either be assimilated into the model to correct model errors. Indeed, a small number of recent studies have begun to quantify the benefits of such a mission for land surface hydrology. For this purpose, synthetic water elevation data were created using the JPL Instrument Simulator (Rodriguez and Moller, 2004) and assimilated into CHS systems (Durand et al., 2008; Biancamaria et al., 2010). In all of these studies, the assimilation of synthetically generated SWOT measurements helped to reduce model errors and improved river discharge simulation. Other studies have used SWOT simulated data as inputs in

HESSD
8, 9173–9227, 2011

algorithms to obtain estimates of river depth and discharge (Durand et al., 2010; Biancamaria et al., 2010). These preliminary results are promising and show the current need for such a mission, and the potential for improving the representation of hydrological processes in current models. Consequently, the next step of this work will consist of using synthetic SWOT data into a suitable assimilation system and to determine their impact on the simulated discharge.

Appendix A

The TRIP river discharge and groundwater outflow

The river discharge simulated by TRIP (Eq. 1) is computed using a streamflow variable velocity, v ($\mathrm{m\,s^{-1}}$), and via the Manning's formula:

$$Q_{\mathrm{out}}^{\mathrm{S}} = \frac{v}{L} S \quad \text{with} \quad v = \frac{\kappa}{n_{\mathrm{riv}}} R^{2/3} s^{1/2} \tag{A1}$$

where L (m) is the river length that takes into account a meandering ratio of 1.4 as proposed by Oki and Sud (1998), s ($\mathrm{m\,m^{-1}}$) is the downstream river height loss per unit length approximated as the river bed slope, R (m) the hydraulic radius, κ ($\mathrm{m^{-3}\,s^{-1}}$) a constant equal to 1, and n_{riv} the dimensionless Manning friction factor which varies from the upstream part to the mouth of each basin. The hydraulic radius is related to the stream water depth, h_{s} (m), calculated from the stream water mass, S (kg), assuming a rectangular river cross-section (Arora and Boer, 1999):

$$R = \frac{W\ h_{\mathrm{s}}}{W + 2\,h_{\mathrm{s}}} \quad \text{where} \quad h_{\mathrm{s}} = \frac{S}{L\,W \rho_{\mathrm{w}}} \tag{A2}$$

where ρ_{w} ($\mathrm{kg\,m^{-3}}$) is the water density, and W (m) the bankfull river width.

HESSD
8, 9173–9227, 2011
Characterization of the hydrological functioning of the Niger basin
V. Pedinotti et al.

The TRIP groundwater outflow (Eq. 1) is computed using the following simple linear relationship proposed by Arora and Boer (1999):

$$Q_{out}^{G} = \frac{G}{\tau} \tag{A3}$$

where τ (s) is an uniform and constant time delay factor of the groundwater reservoir which is fixed to 30 days. This groundwater reservoir does not represent the groundwater dynamics but only delays the groundwater flow contribution to the surface river reservoir within a particular grid cell: the deep drainage is fed into the surface reservoir with a time delay factor of τ. More details can be found in Decharme et al. (2010).

Appendix B

The ISBA-TRIP flood model

As shown in Fig. 1, a simplified rectangular geometry is assumed in TRIP to represent the cross section between the floodplain and the river reservoirs in each grid cell. River flooding arises when the water height of the stream reservoir is higher than the critical bankfull height, h_c (m), and the flood outflow and inflow from this reservoir (Eq. 1) are given by:

$$\left| \begin{array}{l} Q_{in}^{F} = \frac{v_{in}}{W + W_f} M_f \\ Q_{out}^{F} = \frac{v_{out}}{W + W_f} \min\left(M_f, F\right) \end{array} \right. \tag{B1}$$

where W_f (m) is the floodplain width (Appendix A), and M_f (kg) the potential inflow (positive M_f) or outflow (negative M_f) assuming an equilibrium state between the stream and the floodplain water depth:

$$M_f = \rho_W L_f W \left(h_s - h_c - h_f\right) \tag{B2}$$

HESSD
8, 9173–9227, 2011

Characterization of the hydrological functioning of the Niger basin

V. Pedinotti et al.

where L_f (m) and h_f (m) are the length along the river and the depth of the floodplains, h_s (m) the water height of the stream reservoir, and h_c (m) the critical bankfull river height. $W + W_f$ represents the distance covered by M_f from the stream to the floodplains or conversely. v_{in} and v_{out} (m s^{-1}) are the flood inflow and outflow velocities computed using the Manning's formula:

$$v_{in,out} = \frac{s_{in,out}^{1/2}}{n_f} R_{in,out}^{2/3} \qquad \text{(B3)}$$

where n_f is the Manning roughness coefficient for the floodplains that varies according to the vegetation type (Decharme et al., 2011) while $s_{in,out}$ (m m^{-1}) and $R_{in,out}$ (m) are the inflow (or outflow) slope and hydraulic radius respectively at the interface between the floodplain and the river stream.

Finally, the precipitation interception by the floodplains, P_f, the re-infiltration, I_f , and the direct free water surface evaporation, E_f, (Eq. 1) are estimated by ISBA. I_f occurs if the flooded fraction, f_{flood}, calculated according to the subgrid topography (Decharme et al., 2011) is superior to the soil saturated fraction, f_{sat}, and depends on the soil maximum infiltration capacity. In other words, the floodplains cannot infiltrate the fraction of the grid-cell for which the soil is saturated. To a first approximation, it allows to simply represent the fact that the actual floodplains evolve according to the presence of shallow aquifer and water table depth variations. More details can be found in Decharme et al. (2011).

Acknowledgements. This work is supported by the African Monsoon Multidisciplinary Analysis (AMMA) project and the Surface Water Ocean Topography (SWOT) satellite mission project of the "Centre National d'Etudes Spatiales" (CNES). The diverse studies presented in this paper would not have been possible without the valuable contribution of the "Autorité du Bassin du Niger" (ABN), Luc Descroix from the "Laboratoire d'Etudes des Transferts en Hydrologie et Environnement" (LTHE) and Catherine Prigent from the "Laboratoire d'Etudes du Rayonnement et de la Matière en Astrophysique".

The publication of this article is financed by CNRS-INSU.

References

Alkama, M. R., Kageyama, M., Ramstein, G., Marti, O., Ribstein, P., and Swingedouw, D.: Impact of a realistic river routing in coupled ocean-atmosphere simulations of the Last Glacial Maximum climate, Clim. Dynam., 30, 855–869, 2008.

Alkama, R., Decharme, B., Douville, H., Becker, M., Cazenave, A., Sheffield, J., Voldoire, A., Tyteca, S., and Le Moigne, P.: Global evaluation of the ISBA/TRIP continental hydrological system, Part 1: Comparison to GRACE terrestrial water storage estimates and in situ river discharges, J. Hydrometeorol., 11, 583–600, 2010.

Alsdorf, D. E., Rodriguez, E., and Lettenmaier, D. P.: Measuring surface water from 593 space, Rev. Geophys., 45, RG2002, doi:10.1029/2006RG000197, 2007.

Andersen, I., Dione, O., Jarosewich-Holder, M., and Olivry, J. C.: The Niger river basin: A vision for sustainable management, World Bank Publications, 2005.

Andreadis, K. M., Clark, E. A., Lettenmaier, D. P., and Alsdorf, D. E.: Prospects for river discharge and depth estimation through assimilation of swath-altimetry into a raster-based hydrodynamics model, Geophys. Res. Lett., 34, L10403, doi:10.1029/2007GL029721, 2007.

Arora, V. K. and Boer, G. J.: A variable velocity flow routing algorithm for GCMs, J. Geophys. Res., 104, 30965–30979, doi:10.1029/1999JD900905, 1999.

Beven, K. J. and Kirkby, M. J.: A physically-based variable contributing area model of basin hydrology, Hydrol. Sci. Bull., 24, 43–69, 1979.

Biancamaria, S.; K.M. Andreadis., M. Durand, E.A. Clark, E. Rodriguez, N.M. Mognard, D.E. Alsdorf, D.P. Lettenmaier, Y. Oudin, (2010), Preliminary Characterization of SWOT Hydrology Error Budget and Global Capabilities, IEEE Journal of Selected Topics in

HESSD

8, 9173–9227, 2011

Characterization of the hydrological functioning of the Niger basin

V. Pedinotti et al.

Title Page
Abstract | Introduction
Conclusions | References
Tables | Figures
◂ | ▸
Back | Close
Full Screen / Esc
Printer-friendly Version
Interactive Discussion

Applied Earth Observations and Remote Sensing, Volume 3, Issue 1, pp.6-19, 10.1109/JSTARS.2009.2034614.

Biancamaria, S., Durand, M., Andreadis, K. M., Bates, P. D., Boone, A., Mognard, N. M., Rodriguez, E., Alsdorf, D. E., Lettenmaier, D. P., and Clark, E. A.: Assimilation of virtual wide swath altimetry to improve Arctic river modeling, Remote Sens. Environ., 115, 373–381, 2011.

Boone, A., Calvet, J.-C., and Noilhan, J.: Inclusion of a Third Soil Layer in a Land-Surface Scheme using the Force-Restore method, J. Appl. Meteorol., 38, 1611–1630, 1999.

Bonan, G. B.: Sensitivity of a GCM to inclusion of inland water surfaces, J. Climate, 8, 2691–2704, doi:10.1175/1520-0442(1995)008<2691:SOAGST>2.0.CO;2, 1995.

Boone, A., de Rosnay, P., Basalmo, G., Beljaars, A., Chopin, F., Decharme, B., Delire, C., Ducharne, A., Gascoin, S., Grippa, M., Guichard, F., Gusev, Y., Harris, P., Jarlan, L., Kergoat, L., Mougin, E., Nasonova, O., Norgaard, A., Orgeval, T., Ottlé, C., Poccard-Leclercq, I., Polcher, J., Sandholt, I., Saux-Picart, S., Taylor, C., and Xue, Y.: The AMMA Land Surface Model Intercomparison Project, B. Am. Meteorol. Soc., 90, 1865–1880, doi:10.1175/2009BAMS2786.1, 2009.

Bousquet, P., Ciais, P., Miller, J. B., Dlugokencky, E. J., Hauglustaine, D. A., Prigent, C., Van der Werf, G. R., Peylin, P., Brunke, E. G., Carouge, C., Langenfelds, R. L., Lathiere, J., Papa, F., Ramonet, M., Schmidt, M., Steele, L. P., Tyler, S. C., and White, J.: Contribution of anthropogenic and natural sources to atmospheric methane variability, Nature, 443, 439–443, doi:10.1038/nature05132, 2006.

Calmant, S., Seyler, F., and Cretaux, J. F.: Monitoring Continental Surface Waters by Satellite Altimetry, Surv. Geophys., special issue on Hydrology from Space, 29, 247–269, 2008.

Coe, M. T.: A linked global model of terrestrial processes: Simulation of modern rivers, lakes and wetlands, J. Geophys. Res., 103, 8885–8899, 1998.

Coe, M. T.: Modeling terrestrial hydrological systems at the continental scale: Testing the accuracy of an atmospheric GCM, J. Climate, 13, 686–704, doi:10.1175/1520-0442(2000)013<0686:MTHSAT>2.0.CO;2, 2000.

Coe, M. T. and Birkett, C. M.: Calculation of river discharge and prediction of lake Height from satellite radar altimetry: example of the lake Chad basin, Water Resour. Res., 40, W10205, doi:10.1029/2003WR002543, 2004.

Coe, M. T., Costa, M. H., and Howard, E. A.: Simulating the surface waters of the Amazon River basin: impact of new river geomorphic and flow parameterizations, Hydrol. Proc., 22, 2542–2553, doi:10.1002/hyp.6850, 2008.

Cogley, J. G.: The albedo of water as a function of latitude, Mon. Weather Rev., 107, 775781, doi:10.1175/1520-0493(1979)107<0775:TAOWAA>2.0.CO;2, 1979.

Costa, M. H. and Foley, J. A.: Water balance of the Amazon Basin: Dependence on vegetation cover and canopy conductance, J. Geophys. Res., 102, 973–989, doi:10.1029/97JD01865, 1997.

Dadson, S. J., Ashpole, I., Harris, P., Davies, H. N., Clark, D. B., Blyth, E., and Taylor, C. M. : Wetland inundation dynamics in a model of land surface climate: Evaluation in the Niger inland delta region, J. Geophys. Res., 115, D23114, doi:10.1029/2010JD014474, 2010.

Dai, T. and Labadie, J. W.: River basin network model for integrated water quantity/quality management, J. Water Resour. Pl.-ASCE, Vol. 127, September/October, 2001.

de Rosnay, P., Drusch, M., Boone, A., Balsamo, G., Decharme, B., Harris, P., Kerr, Y., Pellarin, T., Polcher, J., and Wigneron, J.-P. : AMMA Land Surface Model Intercomparison Experiment coupled to the Community Microwave Emission Model: ALMIP-MEM, J. Geophys. Res., 114, D05108, doi:10.1029/2008JD010724, 2009.

Decharme, B.: Influence of runoff parameterization on continental hydrology: Comparison between the Noah and the ISBA land surface models, J. Geophys. Res., 112, D19108, doi:10.1029/2007JD008463, 2007.

Decharme, B. and Douville, H. : Introduction of a sub-grid hydrology in the ISBA land surface model, Clim. Dynam., 26, 65–78, 2006.

Decharme, B., Douville, H., Boone, A., Habets, F., and Noilhan, J.: Impact of an exponential profile of saturated hydraulic conductivity within the ISBA LSM: simulations over the Rhône basin, J. Hydrometeorol., 7, 6180, 2006.

Decharme, B., Douville, H., Prigent, C., Papa, F., and Aires, F. : A new river flooding scheme for global climate applications: Offline evaluation over South America, J. Geophys. Res., 113, D11110, doi:10.1029/2007JD009376, 2008.

Decharme, B., Alkama, R., Douville, H., Becker, M., and Cazenave, A. : Global evaluation of the ISBA-TRIP continental hydrological system, Part II: Uncertainties in river routing simulation related to flow velocity and groundwater storage, J. Hydrometeorol., 11, 601–617, 2010.

Decharme, B., Alkama, R., Papa, F., Faroux, S., Douville, H., and Prigent, C.: Global off-line evaluation of the ISBA-TRIP flood model, Clim. Dynam., doi:.10.1007/s00382-011-1054-9, in press, 2011.

Descroix, L., Mahé, G., Lebel, T., Favreau, G., Galle, S., Gautier, E., Olivry, J. C., Albergel, J., Amogu, O., Cappelaere, B., Dessouassi, R., Diedhiou, A., Le Breton, E., Mamadou, I., and Sighomnou, D.: Spatio-temporal variability of hydrological regimes around the boundaries between Sahelian and Sudanian areas of West Africa: A synthesis, J. Hydrol., 375, 9010, doi:10.1016/j.jhydrol.2008.12.012, 2009.

Dirmeyer, P. A., Gao, X., Zhao, M., Guo, Z., Oki, T., and Hanasaki, N.: GSWP-2: Multimodel analysis and implications for our perception of the land surface, B. Am. Meteorol. Soc., 87, 1381–1397, 2006.

Douville, H., Planton, S., Royer, J. F., Stephenson, D. B, Tyteca, S., Kergoat, L., Lafont, S., and Betts, R. A.: Importance of vegetation feedbacks in doubled-CO2 climate experiments, J. Geophys. Res.,105, 14841–14861, 2000.

Dunn, C. E., Bertiger, W., Bar-Sever, Y., Desai, S., Haines, B., Kuang, D., Franklin, G., Harris, I., Kruizinga, G., Meehan, T., Nandi, S., Nguyen, D., Rogstad, T., Thomas, J. B., Tien, J., Romans, L., Watkins, M., Wu, S.-C., Bettadpur, S., and Kim, J.: Instrument of GRACE:GPS augments gravity measurements, application challenge, GPS World, 2003.

Durand, M., Andreadis, K. M., Alsdorf, D. E., Lettenmaier, D. P., Moller, D., and Wilson, M.: Estimation of bathymetric depth and slope from data assimilation of swath altimetry into a hydrodynamic model, Geophys. Res. Lett., 35, L20401, doi:10.1029/2008GL034150, 2008.

Durand, M., Rodriguez, E., Alsdorf, D. E., and Trigg, M.: Estimating River Depth From Remote Sensing Swath Interferometry Measurements of River Height, Slope, and Width, IEEE J. Sel. Top. in Appl., 3, 20–31, doi:10.1109/JSTARS.2009.2033453, 2010.

Fontes, J.-C., Andrews, J. N., Edmunds, W. M., Guerre, A., and Travi, Y.: Paleorecharge by the Niger River (Mali) deduced from groundwater geochemistry, Water Resour. Res., 27, 199–214, 1991.

Gedney, N., Cox, P. M., Douville, H., Polcher, J., and Valdes, J. P.: Characterizing GCM land surface schemes to understand their responses to climate change, J. Climate, 13, 3066–3079, 2000.

Geiger, B., Meurey, C., Lajas, D., Franchistéguy, L., Carrer, D., and Roujean, J-.L.: Near real-time provision of downwelling shortwave radiation estimates derived from satellite observations, Meteorol. Appl., 15, 411–420, 2008.

Getirana, A. C. V., Bonnet, M.-P., Rotunno, O. C., Collischonn, W., Guyot, J. L., Seyler, F., and Mansur, W. J.: Hydrological modelling and water balance of the Negro River basin: evaluation based on in situ and spatial altimetry data, Hydrol. Process., 24, 3219–3236, 2010.

Grippa, M., Mognard, N. M., Letoan, T., and Josberger, E. G.: Siberia snow depth climatology from SSM/I data using a combined dynamic and static algorithm, Remote Sens. Environ., 93, 3041, 2004.

Grippa, M., Kergoat, L., Frappart, F., Araud, Q., Boone, A., de Rosnay, P., Lemoine, J.-M., Gascoin, S., Balsamo, G., Ottlé, C., Decharme, B., Saux-Picart, S., and Ramillien, G.: Land water storage variability over West Africa estimated by GRACE and land surface models, Water Resour. Res., in press, 2011.

Habets, F., Boone, A., Champeaux, J.-L., Etchevers, P., Franchistéguy, L., Leblois, E., Ledoux, E., Le Moigne, P., Martin, E., Morel, S., Noilhan, J., Quintana Seguì, P., Rousset-Regimbeau, F., and Viennot, P.: The SAFRAN-ISBA-MODCOU hydrometeorological model applied over France, J. Geophys. Res., 113, D06113, doi:10.1029/2007JD008548, 2008.

Houweling, S., Kaminski, T., Dentener, F., Lelieveld, J., and Heinmann, M.: Inverse modeling of methane sources and sinks using adjoint of a global transport model, J. Geophys. Res., 104, 26137–26160, doi:10.1029/1999JD900428, 1999.

Huffman, G. J., Adler, R. F., Bolvin, D. T., Gu, G., Nelkin, E. J., Bowman, K. P., Hong, Y., Stocker, E. F., and Wolff, D. B.: The TRMM Multisatellite Precipitation Analysis (TMPA): Quasiglobal, multiyear, combined-sensor precipitation estimates at fine scales, J. Hydrometeorol., 8, 3855, 2007.

Knighton, E.: Fluvial forms and processes: A new perspective, Edward Arnold, London, p.383, 1998.

Lawrence, D. M. and Slater, A. G.: Incorporating organic soil into a global climate model, Clim. Dynam., 30, 145–160, 2007.

Laws, K. B., Janowiak, J. E., and Huffman, J. G.: Verification of rainfall estimates over Africa using RFE, NASA MPA-RT and CMORPH, AMS 18th Conference on Hydrology, Seattle, Washington, 2004.

Lee, H., Durand, M., Jung, H. C., Alsdorf, D., Shum, C. K., and Sheng, Y.: Characterization of surface water storage changes in Arctic lakes using simulated SWOT measurements, Int. J. Remote Sens., 31, 3931–3953, 2010.

Lehner, B. and Döll, P.: Developement and validation of a global database of lakes, reservoirs and wetlands, J. Hydrol., 296, 1–22, 2004.
Leon, J. G., Calmant, S., Seyler, F., Bonnet, M.-P., Cauhopé, M., Frappart, F., Filizola, N., and Fraizy, P.: Rating curves and estimation of average water depth at the upper Negro River based on satellite altimeter data and modeled discharges, J. Hydrol., 328, 481–496, 2008.
Leopold, L. B., Wolman, M. G., and Miller, J. P.: Fluvial Processes in Geomorphology, W. H. Freeman, New York, 1964.
Llovel, W., DoMinh, K., Cazenave, A., Cretaux, J.-F., Gennero, M. C., and Becker, M.: Contribution of land water storage change to global mean sea level from GRACE and satellite altimetry, C. R. Geosci., 342, 179–188, doi:10.1016/j.crte.2009.12.004, 2010.
Lunetta, R. S., Knight, J. F., Ediriwickrema, J., Lyon, J. G., and Worthy, L. D.: Land-cover change detection using multi-temporal MODIS NDVI data, Remote Sens. Environ., 105, 142–154, 2006.
Lyon, J. G., Yuan, D., Lunetta, R. S., and Elvidge, C. D.: A change detection experiment using vegetation indices, Photogramm. Eng. Remote Sens., 64, 143–150, 1998.
Mahe, G., Bamba, A., Soumaguel, A., Orange, D., and Olivry, J.-C.: Water losses in the inner delta of the River Niger: water balance and flooded area, Hydrol. Process., 23, 3157–3160, doi:10.1002/hyp.7389, 2009.
Matthews, E.: Wetlands, in Atmospheric Methane: Its Role in the Global Environment, edited by: Khalil, M. A. K., Springer, New York, 202–233, 2000.
Meynadier, R., Bock, O., Guichard, F., Boone, A., Roucou, P., and Redelsperger, J.-L.: The West African Monsoon water cycle. Part I: a hybrid water budget dataset, J. Geophys. Res., 115, D19106, doi:10.1029/2010JD013917, 2010.
Miller, J. R., Russell, G. L., and Caliri, G.: Continental scale river flow in climate models, J. Climate, 7, 914–928, doi:10.1175/1520-0442(1994)007<0914:CSRFIC>2.0.CO;2, 1994.
Molod, A., Salmun, H., and Waugh, D.: The Impact on a GCM Climate of an Extended Mosaic Technique for the Land – Atmosphere Coupling, J. Climate, 17, 3877–3891, 2004.
Moody, J. A. and Troutman, B. M.: Characterization of the spatial variability of channel morphology, Earth Surf. Proc. Land., 27, 1251–1266, 2002.
Noilhan, J. and Planton, S.: A simple parameterization of land surface processes for meteorological models, Mon. Weather Rev., 117, 536–549, doi:10.1175/1520-0493(1989)117<0536:ASPOLS>2.0.CO;2, 1989.

HESSD
8, 9173–9227, 2011

Oki, T. and Sud, Y. C.: Design of total runoff integrating pathways (TRIP), Earth Interact., 2, 136, doi:10.1175/1087-3562(1998)002<0001:DOTRIP>2.3.CO;2, 1998.

Oki, T., Nishimura, T., and Dirmeyer, P.: Assessment of annual runoff from land surface models using Total Runoff Integrating Pathways (TRIP), J. Meteorol. Soc. Jpn., 77, 235–255, 1999.

Papa, F., Guntner, A., Frappart, F., Prigent, C., and Rossow, W. B.: Variations of surface water extent and water storage in large river basins: A comparison of different global data sources, Geophys. Res. Lett., 35, L11401, doi:10.1029/2008GL033857, 2008.

Papa, F., Durand, F., Rossow, W. B., Rahman, A., and Bala, S. K.: Satellite altimeter derived monthly discharge of the Ganga Brahmaputra River and its seasonal to interannual variations from 1993 to 2008, J. Geophys. Res., 115, C12013, doi:10.1029/2009JC006075, 2010a.

Papa, F., Prigent, C., Aires, F., Jimenez, C., Rossow, W. B., Matthews, E.: Interannual variability of surface water extent at the global scale, 1993–2004 , J. Geophys. Res.-Atmos., 115, D12111, doi:10.1029/2009JD012674, 2010b.

Pierre, C., Bergametti, G., Marticorena, B., Mougin, E., Lebel, T., and Ali, A.: Pluriannual comparisons of satellite based rainfall products over the Sahelian belt for seasonal vegetation modelling, J. Geophys. Res., doi:10.1029/2011JD016115, in press, 2011.

Prigent, C., Matthews, E., Aires, F., and Rossow, W. B.: Remote sensing of global wetland dynamics with multiple satellite data set, Geophys. Res. Lett., 28, 4631–4634, 2001.

Prigent, C., Papa, F., Aires, F., Rossow, W. B., and Matthews, E.: Global inundation dynamics inferred from multiple satellite observations, 1993–2000, J. Geophys. Res., 112, D12107, doi:10.1029/2006JD007847, 2007.

Redelsperger, J.-L., Thorncroft, C. D., Diedhiou, A., Lebel, T., Parker, D. J., and Polcher, J.: African Monsoon Multidisciplinary Analysis: An international research project and field campaign, B. Am. Meteorol. Soc., 87, 1739–1746, 2006.

Roddel, M., Velicogna, I., and Famiglietti, J. S.: Satellite-based estimates of groundwater depletion in India, Nature, 460, 999–1003, doi:10.1038/nature08238, 2009.

Rodriguez, E.: SWOT science requirements Document, JPL document, Initial release, 2004.

Rodriguez, E. and Moller, D.: Measuring surface water from space, Eos Trans. AGU, 85, Fall Meet. Suppl., Abstract H22C-08, 2007.

Sausen, R., Schubert, S., and Dumenil, L.: A model of river runoff for use in coupled atmosphere ocean models, J. Hydrol. Amsterdam, 155, 337–352, doi:10.1016/0022-1694(94)90177-5, 1994.

Sheffield, J., Goteti, G., and Wood, E. F.: Development of a 50-year high-resolution global data set of meteorological forcings for land surface modeling, J. Climate, 19, 3088–3111, 2006.
Swenson, S., Wahr, J., and Milly, P.: Estimated accuracies of regional water storage variations inferred from the Gravity Recovery and Climate Experiment (GRACE), Water Resour. Res., 39, 1223, doi:10.1029/2002WR001808, 2003.
Taylor, C. M.: Feedbacks on precipitation from an African wetland, Geophys. Res. Lett., 37, L05406, doi:10.1029/2009GL041652, 2010.
Taylor, C. M., Gounou, A., Guichard, F., Harris, P. P., Ellis, R. J., Couvreux, F., and De Cauwe, M.: Frequency of Sahelian storm initiation enhanced over mesoscale soil-moisture patterns, Nat. Geosci., 4, 430–433, doi:10.1038/ngeo1173, 2011.
Vorosmarty, C. J., Moore III, B., Grace, A. L., Gildea, M. P., Melillo, J. M., Peterson, B. J., Rastetter, E. B., and Steudler, P. A.: Continental scale models of water balance and fluvial transport: An application to South America, Global Biogeochem. Cy., 3, 241–265, doi:10.1029/GB003i003p00241, 1989.
Vouillamoz, J. M., Favreau, G., Massuel, S., Boucher, M., Nazoumou, Y., and Legchenko, A.: Contribution of magnetic resonance to aquifer characterization and recharge estimate in semiarid Niger, J. Appl. Geophys., 64, 99–108, doi:10.1016/j.jappgeo.2007.12.2006, 2007.
Wahr, J., Swenson, S., Zlotnicki, V., and Velicogna, I.: Timevariable gravity from GRACE: First results, Geophys. Res. Lett., 31, L11501, doi:10.1029/2004GL019779, 2004.
Wigneron, J. P., Calvet, J. C., Pellarin, T., Van de Griend, A., Berger, M., and Ferrazzoli, P.: Retrieving near-surface soil moisture from microwave radiometric observations: current status and future plans, Remote Sens. Environ., 85, 489–506, 2003.
Zagona, E. A., Fulp, T. J., Shane, R., Magee, T., and Goranflo, H. M.: RiverWare: A generalized too–929, doi:10.1111/j.1752-1688.2001.tb05522.x, 2001.

HESSD
8, 9173–9227, 2011

Characterization of the hydrological functioning of the Niger basin

V. Pedinotti et al.

Table 1. Threshold values used for the classification surface type used to monitor flood events. Band unit of reflectance is internal HDF-EOS data format specific to the Modis data and do not correspond to usual reflectance unit.

	Open water	Mix water/Dry land	Aquatic vegetation	Vegetation	Dry land
Band 5	<1200	>1200 & <2700	>1200 & <2700	>2700	>2700
NDVI	No test	<0.4	>0.4	>0.4	<0.4

HESSD
8, 9173–9227, 2011

Table 2. ISBA/TRIP key input parameters and the variations applied for sensitivity tests.

Case 1	h_c	Spatially distributed constant in time	a. +20 % b. −20 %
Case 2	W	Spatially distributed constant in time	a. +20 % b. −20 %
Case 2	n_{riv}	Spatially distributed constant in time	a. +20 % b. −40 %
Case 4	τ	Constant in space and time	$\tau = 60$; 90
Case 5	τ_{aq}	Constant in space and time	$\tau_{aq} = 1$; 16

HESSD
8, 9173–9227, 2011

Characterization of the hydrological functioning of the Niger basin

V. Pedinotti et al.

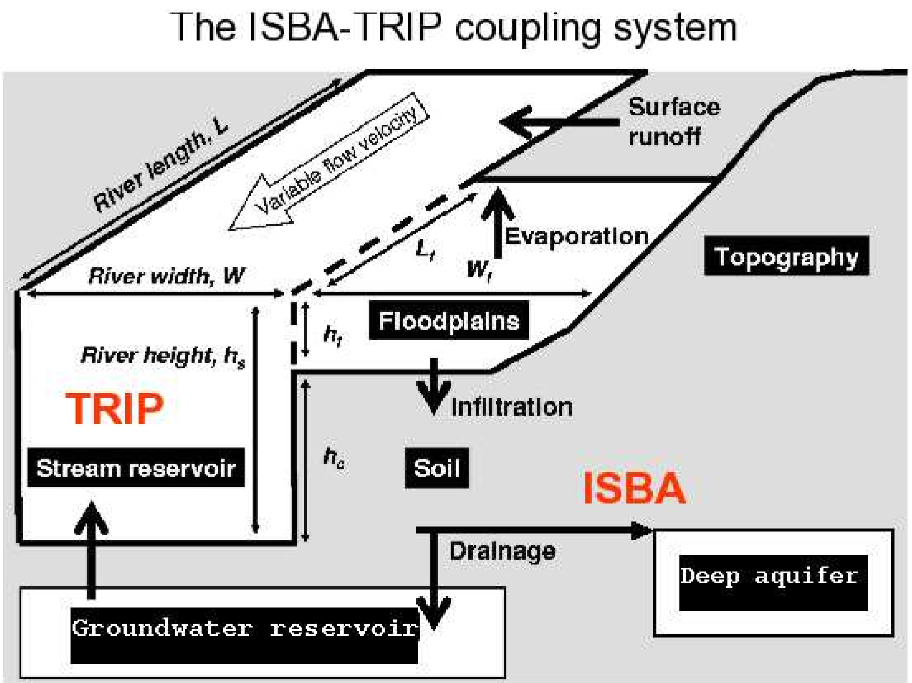

Fig. 1. Schematic representation of the ISBA/TRIP (Oki et al., 1999; Decharme et al., 2007) coupled system. The surface runoff calculated by the land surface model (ISBA) flows into the stream reservoir. The flood dynamic is described using a prognostic flood reservoir which fills when the river height exceeds a critical value and vice versa. The flood fraction is based on sub-grid topography. Finally, we add a linear aquifer reservoir so that the deep drainage is divided between the groundwater and the deep aquifer reservoirs.

HESSD
8, 9173–9227, 2011

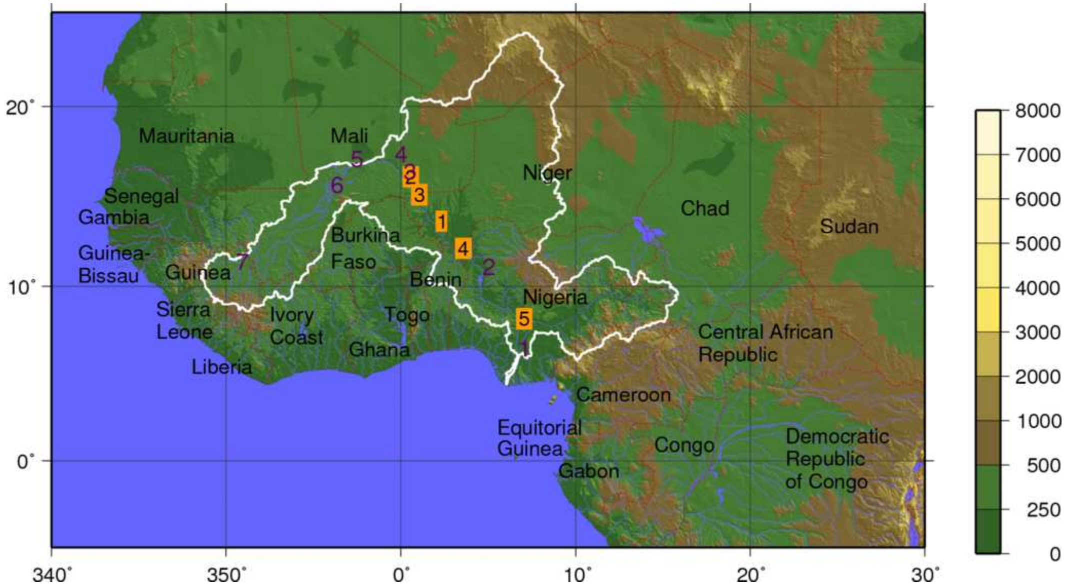

Fig. 2. ALMIP domain (stops at latitude 20° N). The special resolution is 0.5° × 0.5°. The white contour is the delimitation of the Niger basin. The yellow squares are the cities were discharge observations are available: (1) Niamey (2) Ansongo (3) Kandadji (4) Malanville (5) Lokoja The purple figures are the sites where height change observations are used for evaluation.The legend indicates the topographical heights values (m).

HESSD
8, 9173–9227, 2011

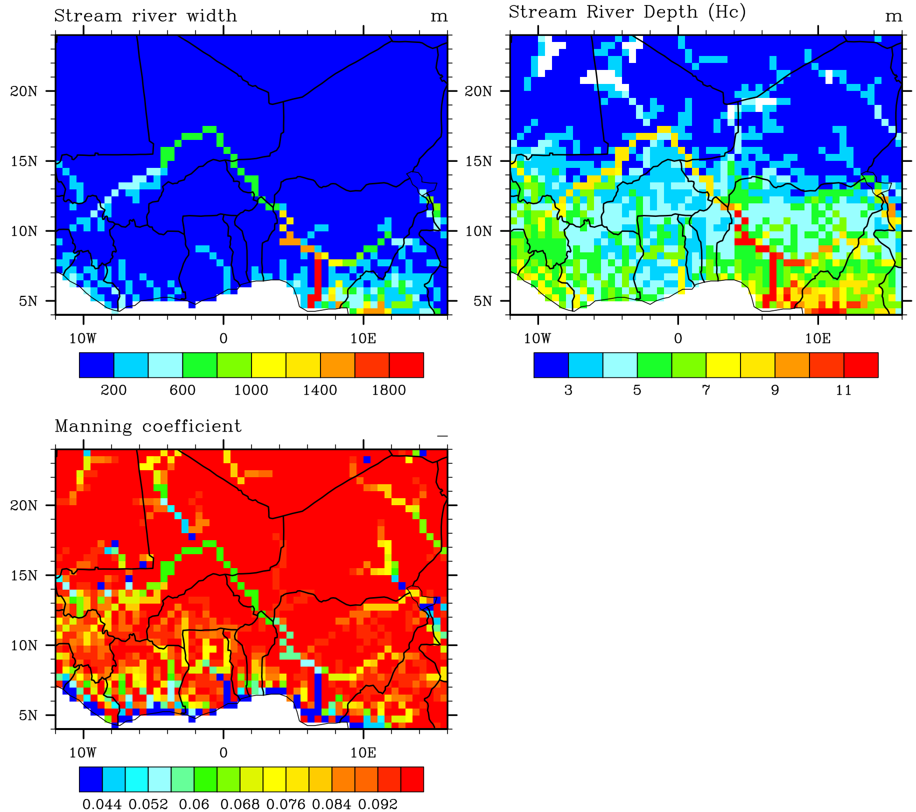

Fig. 3. Some TRIP parameters. Spatial distribution of the river width (up left), the river depth (up right) and the Manning coefficient (down).

HESSD

8, 9173–9227, 2011

Characterization of the hydrological functioning of the Niger basin

V. Pedinotti et al.

Title Page
Abstract | Introduction
Conclusions | References
Tables | Figures
◂I | I▸
◂ | ▸
Back | Close
Full Screen / Esc
Printer-friendly Version
Interactive Discussion

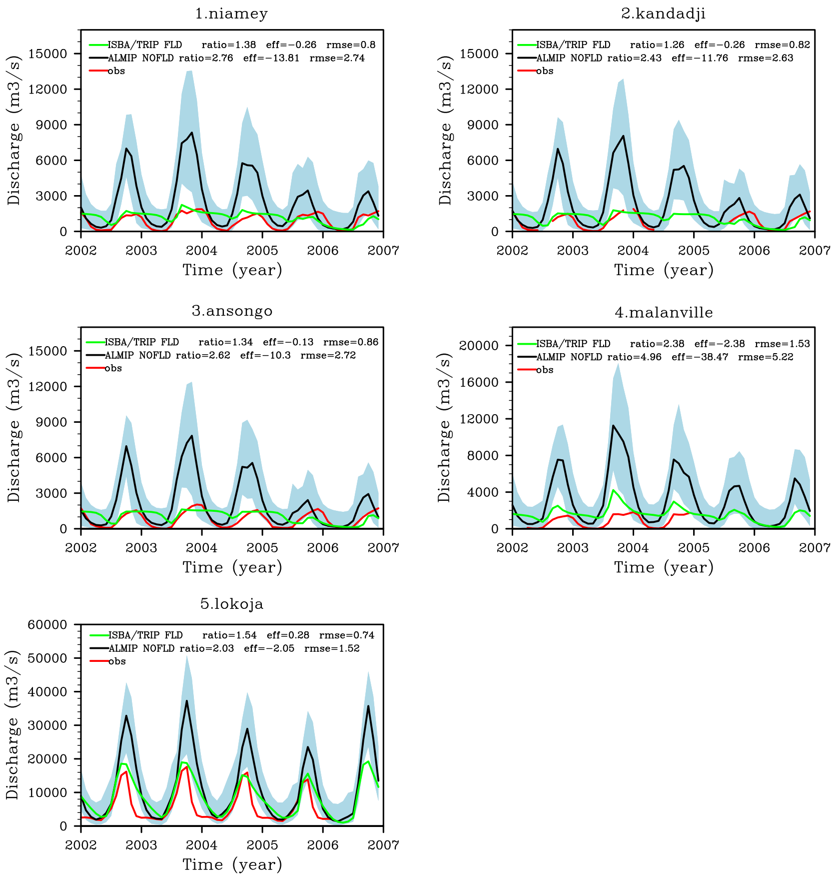

Fig. 4. Monthly discharges (2002–2006) simulated by ALMIP LSMs (average, black line) and by ISBA-TRIP using the flooding scheme (green). Observations are in red and the blue range is limited by the minimum and maximum discharge simulated by LSMs. The TRMM-3B42 rain product is used as forcing input.

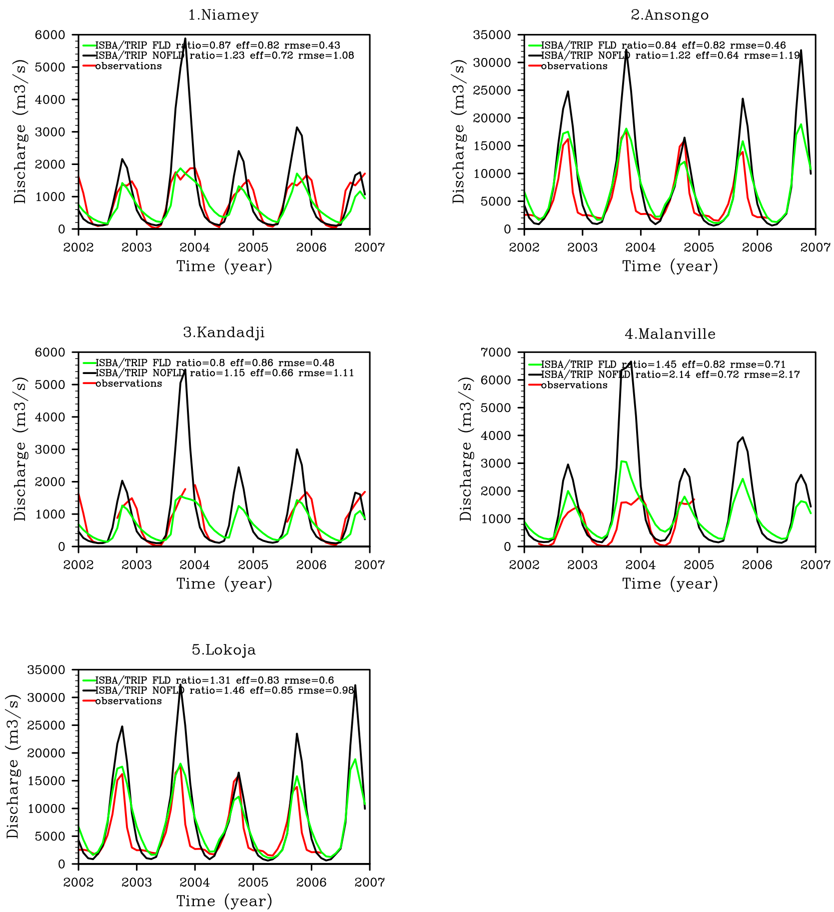

Fig. 5. Monthly discharges (2002–2006) simulated by ISBA-TRIP with (green) and without (black) the flooding scheme. Observations are in red. The RFE2.0 rain product is used as forcing input.

HESSD
8, 9173–9227, 2011

Characterization of the hydrological functioning of the Niger basin

V. Pedinotti et al.

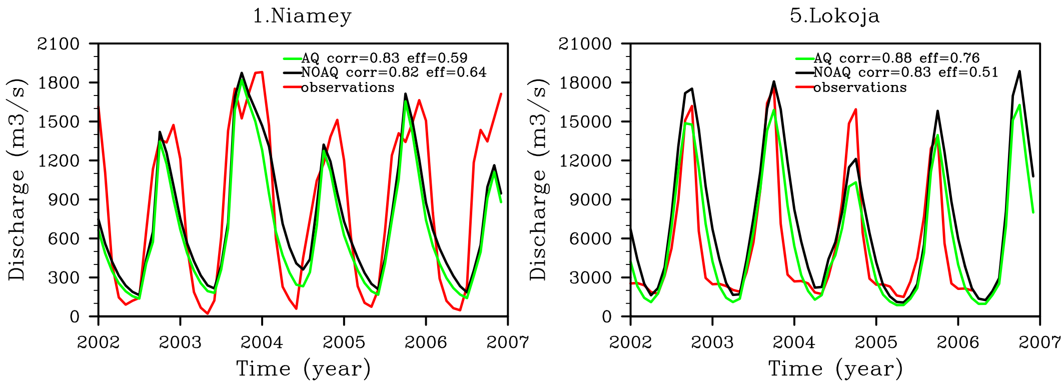

Fig. 6. Monthly discharges (2002–2006) simulated by ISBA-TRIP with (green) and without (black) aquifers in Niamey and Malanville. Observations are in red.

HESSD
8, 9173–9227, 2011
Characterization of the hydrological functioning of the Niger basin
V. Pedinotti et al.

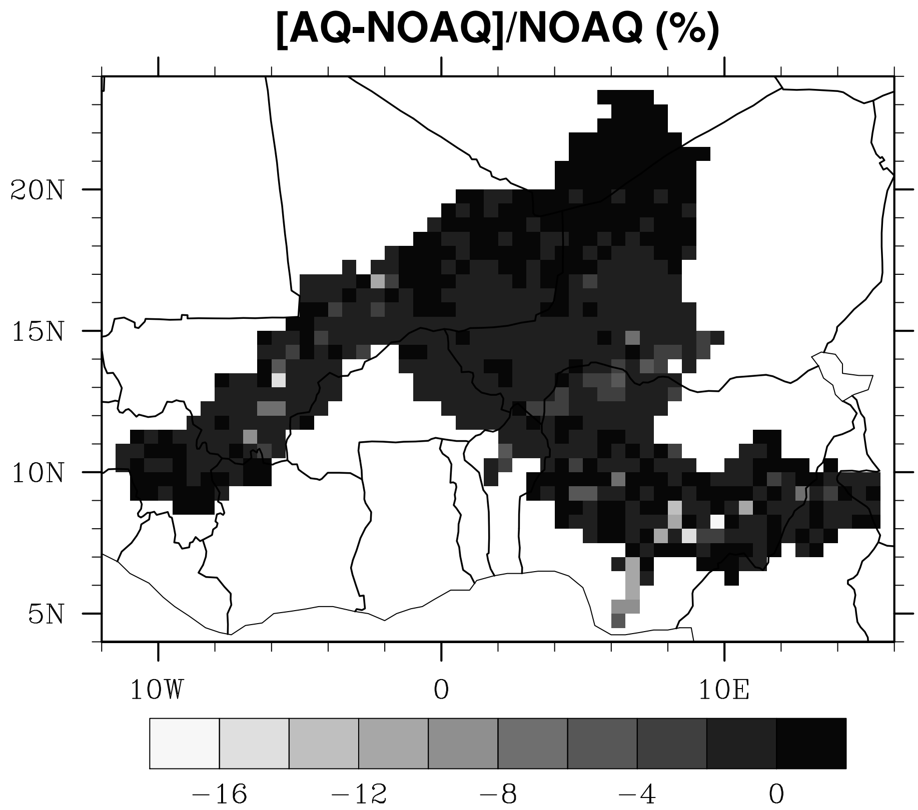

Fig. 7. Spatial distribution of the relative difference ([AQ-NOAQ]/AQ) between the AQ (without aquifers) and the AQ (with aquifers) evaporations (%) averaged for each month over the period 2002–2006 when forced with RFE2.0.

HESSD
8, 9173–9227, 2011

Characterization of the hydrological functioning of the Niger basin

V. Pedinotti et al.

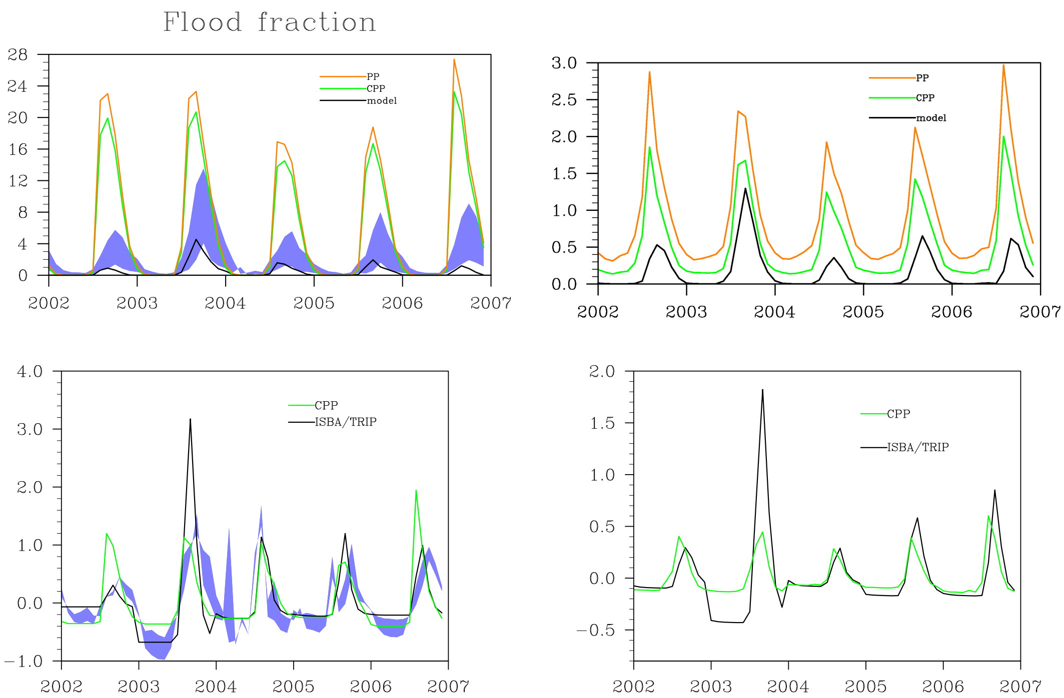

Fig. 8. Time evolution of the mean monthly flooded fraction (in %) respectively averaged over the inner delta region (a, up left) and over the Niger basin (b, up right). The blue range is the interval between the minimum and the maximum Modis classification (JFC) flooded fraction. Time series of deseasonalized flood fraction anomalies (obtained by subtracting the 12-year mean monthly value from individual months and then dividing by the standard deviation) over the delta (c, down left) and over the entire basin (d, down right). The blue range on the left figure delineates the maximum and minimum possible anomalies from Modis (JFC) products. The CPP product is green and ISBA-TRIP is in black. The yellow line is the non-hybridized product.

HESSD
8, 9173–9227, 2011

Title Page
Abstract | Introduction
Conclusions | References
Tables | Figures
◄ | ►
Back | Close
Full Screen / Esc
Printer-friendly Version
Interactive Discussion

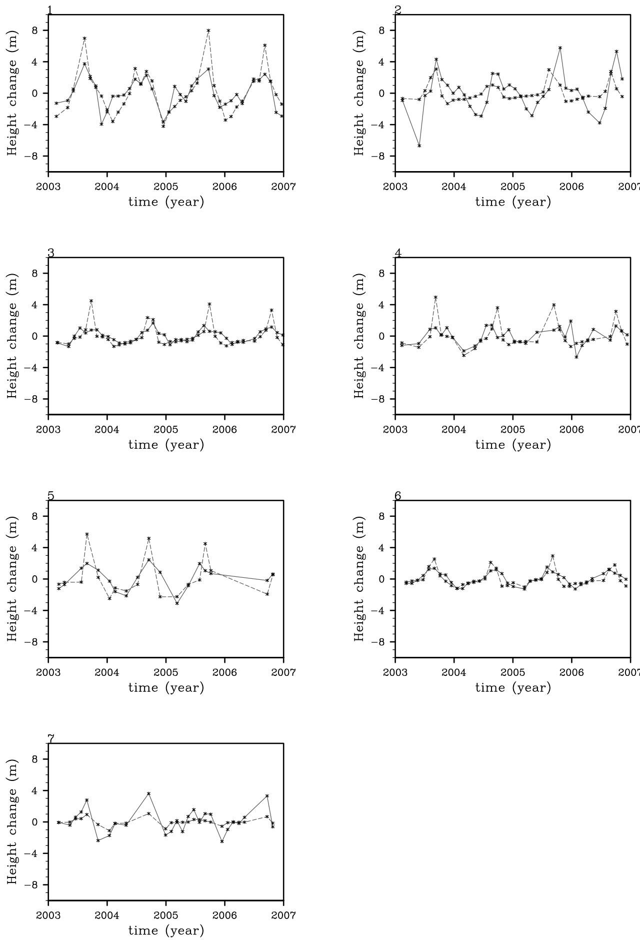

Fig. 9. River height changes in 7 sites along the Niger river. The shaded lines represent the ISBA-TRIP height changes and the full lines are the observations.

HESSD

8, 9173–9227, 2011

Characterization of the hydrological functioning of the Niger basin

V. Pedinotti et al.

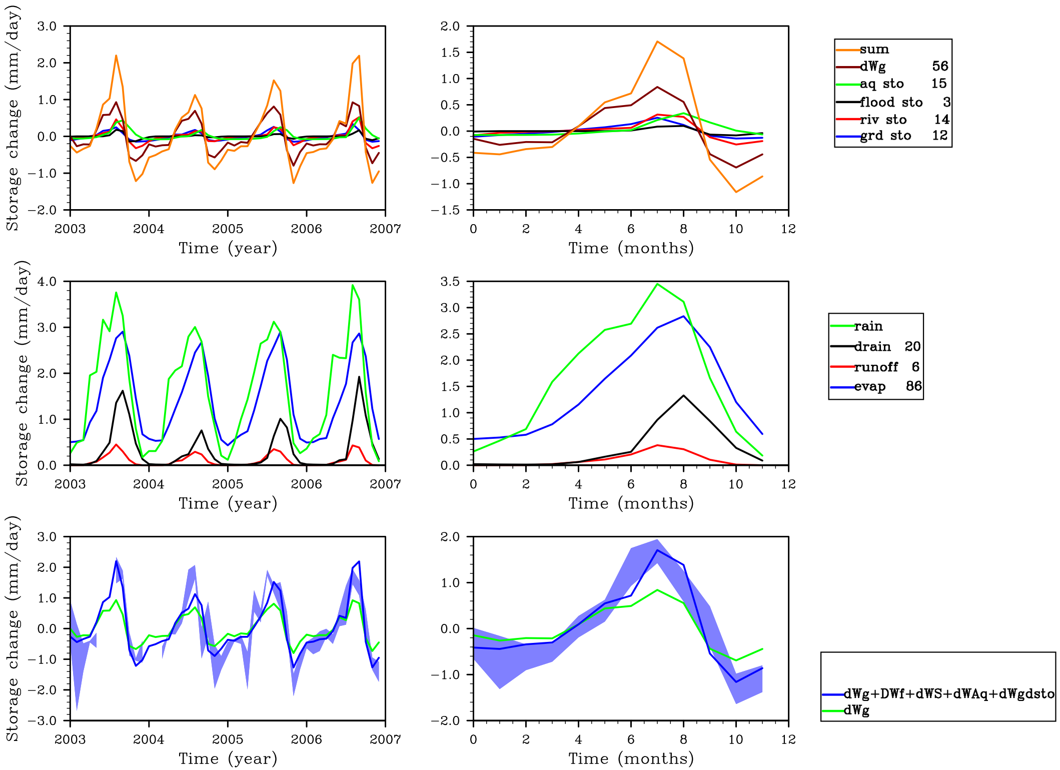

Fig. 10. Basin water storage change (mm day^{-1}) of each reservoir (top). The figures in the legend are the contribution of each reservoir to the total water storage change averaged over the period. Time evolution of rain, runoff, drainage and evaporation over the basin (middle). The figures in the legend are the ratio of each variable over the rain averaged over the period. Basin water storage change (mm day^{-1}) in all reservoirs compared to GRACE datasets (down). The blue range is the difference between the maximum and the minimum GRACE products values. Left panels represent interannual variations (monthly averages) and right panels are the annual variations (each month is average over the whole 4 years period).

HESSD

8, 9173–9227, 2011

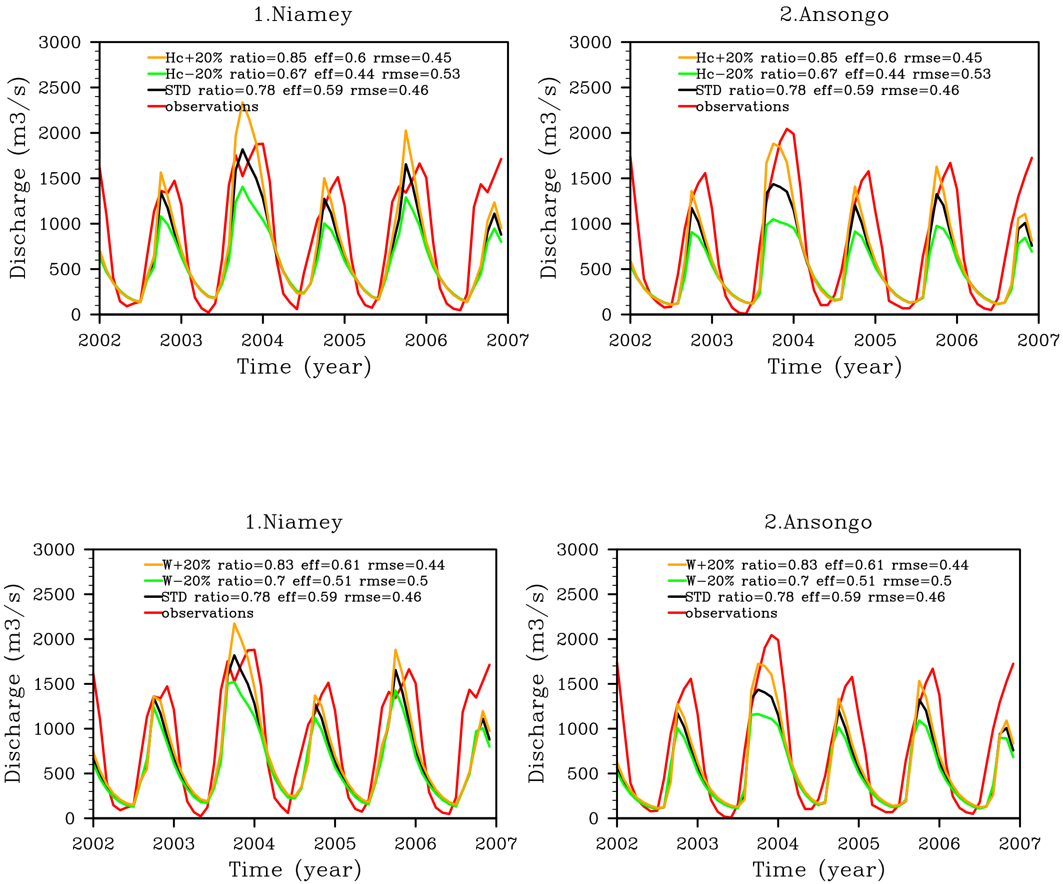

Fig. 11. Impact of modifications of the critical height h_c (a an b, up) and of the river width W (c and d, down) on the monthly.

HESSD
8, 9173–9227, 2011

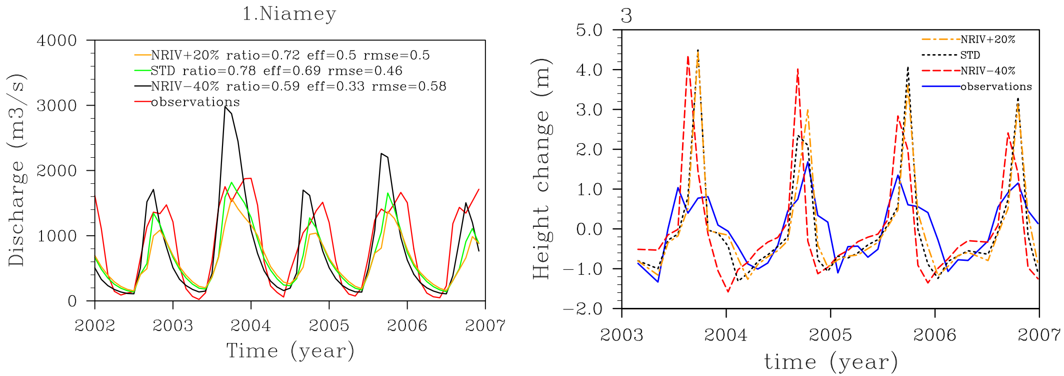

Fig. 12. Impact of the Manning coefficient on the river discharges and on the river height changes.

HESSD
8, 9173–9227, 2011

Characterization of the hydrological functioning of the Niger basin

V. Pedinotti et al.

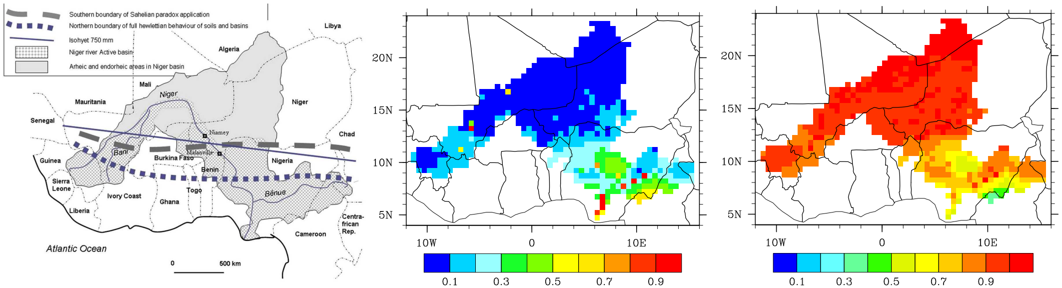

Fig. 13. Left panel: the Niger River Basin (from Descroix et al., 2009) and boundaries of the Sahelian paradox and Hewlettian environments. The 750 mm separates roughly Sahel (northward) and Sudan, between the Upper Niger river basin and the Lake Chad. The active and endorheic parts of the basin are also delineated. Middle panel: ratio of the sum of runoff and drainage from LSM over the precipitation. This ratio is averaged over the period 2002–2006. Right panel: ratio of evaporation over the precipitation, averaged over the period 2002–2006.

HESSD
8, 9173–9227, 2011